Convergence analysis of the direct simulation Monte Carlo based on the physical laws of conservation

A. Karchani and R. S. Myong[1]

Department of Aerospace and System Engineering and Research Center for
Aircraft Parts Technology,
Gyeongsang National University, Jinju, Gyeongnam 660-701, South Korea

Abstract:

Computational errors in the direct simulation Monte Carlo method can be categorized into four types; decomposition (or discretization), statistical, machine, and boundary condition errors. They arise due to variety of reasons including decoupling of movement and collision phases into two separate steps, finiteness of molecule numbers and domain cell-size, existence of statistical fluctuations and uncertainty, using machines to solve physical problems numerically, computational implementation of boundary conditions of approximate nature, and, finally, assumptions and simplifications adopted in the inter-molecular collision models. In this study, a verification method based on the physical laws of conservation, which are an exact consequence of the Boltzmann equation, is introduced in order to quantify the errors of the DSMC method. A convergence history according to the new verification method is then presented that can illustrate the effects of all type of errors during the simulation run. Convergence analysis indicates that the DSMC method can satisfy the conservation laws with an acceptable level of precision for the flow problems studied. Finally, it is shown that the overall deviation from conservation laws increases with decreasing sample size value and number of particles, and with increasing length of cells and time-step interval size.

---

[1] Corresponding author: Tel: +82-55-772-1645.
Email: myong@gnu.ac.kr.

1. Introduction

The kinetic Boltzmann equation is considered the foundation for theoretical studies of rarefied gas flows. However, solving the Boltzmann equation directly in phase space is not an easy task because of the complexity and non-linearity of the collisional term [1]. For this reason, analytical study of the equation has been limited to simple flows. As an alternative, the direct simulation Monte Carlo (DSMC) was introduced by Bird to simulate directly the molecular behavior of non-equilibrium gas flows [2-4]. In the DSMC method, a large number of particles are represented by one simulated particle so that the cost of the DSMC method is considerably lower than the molecular dynamics simulation of particles. Owing to its computational simplicity and accuracy, the DSMC method is now being used in various applications: not only for traditional rarefied hypersonic gas flows, but also for micro-scale gases, material processing, acoustic agglomeration processes, and gaseous mixing [5-10].

Generally, computational errors in the DSMC method can be categorized into four types; decomposition (or discretization), statistical, machine, and boundary condition errors. The four types of error and associated computational parameters are depicted in Fig. 1. The decomposition error arises from decoupling of the motion and collision phases into two segregated steps in the DSMC method. The statistical error is generated due to the statistical nature of the DSMC method. The machine error, so-called 'round-off-error,' is inevitable in any numerical method. However, the machine error can easily be minimized using 64-bit data type variables [11].

In the past, much effort has been devoted to the analysis of decomposition and statistical errors in order to enhance the accuracy of the DSMC method. The decomposition error—the

2

most important type—is basically a function of three computational parameters: time-step (Δt), cell-size (Δx), and the number of particles (N) [3]. As Wagner [12] proved theoretically, the DSMC solution will converge to the solution of Boltzmann equation of *a gas undergoing binary collisions between gas particles*, if the value of these parameters are chosen properly (and when no wall surface boundary condition is involved in the simulation). In passing it must be noted that the Boltzmann theory has not been fully worked out for modifying the collision term that should correctly reflect *the molecular collision with the wall surface atoms*. This—subtle, but often neglected—point has already been noticed by various previous studies like Cercignani [13] and Villani [14], in which it was stated: "*These conservation laws should hold true when there are no boundaries. In presence of boundaries, conservation laws may be violated: momentum is not preserved by specular reflection, neither is energy if the gas is in interaction with a wall kept at a fixed temperature.*" Thus, the DSMC solution of gaseous flow problems (with no wall surface boundary conditions) can be considered a statistical solution of the Boltzmann equation when infinite numbers of particles are used, and when the values of time-step and cell-size approach zero. Nevertheless, the values of time-step and cell-size cannot be taken as infinitesimally small in reality, due to limitation of numerical computation. Consequently, the decomposition error will always exist and influence the accuracy of the DSMC method. Bird [3] presented two conditions that the time-step value must be a fraction of the mean collision time and the cell-size value should be smaller than the mean free path. He also suggested that the number of particles per cell should be greater than 20. Later, Meiburg [15] showed that these parameters need to be examined more carefully in order to yield accurate results.

Many studies have been also conducted to investigate the effects of computational parameters on decomposition error, and to quantify the amount of error associated with them. For example, Alexander et al. [16] studied a one-dimensional stationary problem, in the limit

of infinite number of particles and vanishing time-step value, in order to analyze the role of cell-size on decomposition error. They found that the error comes from the collision pair selection division where particle partners are selected from any place throughout the collision cell. Hadjiconstantinou [17] derived an explicit expression for describing the influence of time-step value on the decomposition error. Garcia et al. [18] compared the measured transport coefficients by DSMC with the results obtained from the Green-Kubo theory. They found that the time-step error is closely connected to re-collision phenomena. Rader et al. [19] compared the value of bulk thermal conductivity calculated by the DSMC simulation with results of the Chapman-Enskog theory. The difference between the DSMC and the theoretical result was found less than 0.2% at a given fine value of computational parameters. Interestingly, they also reported that the convergence behavior of error becomes much more complicated when all three parameters are considered simultaneously. Rader et al. [11] also studied the convergence behavior as function of temperature and heat flux in various configurations of the DSMC algorithms. They found that the computational parameters can affect the accuracy of the high order moment properties (e.g., heat flux), more than the first order moment, conserved, properties (e.g., temperature).

The DSMC method utilizes stochastic numerical procedures; hence, it inherits the statistical features of probabilistic methods such as random fluctuation and statistical uncertainty. Moreover, the probability sampling process is added to filter out statistical uncertainty and to estimate the mean value of the estimators. The statistical error can be, in general, reduced by increasing the sample size. However, the statistical uncertainty will not vanish completely because of the finite sample size in the DSMC process. The sample size is basically a function of number of particles and sample steps. Therefore, the magnitude of statistical error is inversely proportional to the square root of the number of particles and the sample steps [3, 20].

Recently, there have been several studies on the analysis of statistical error in the DSMC method. Mansour et al. [21] estimated the amount of statistical error for temperature variable by considering hydrodynamic fluctuations in dilute gas. Chen et al. [20] analyzed the effect of the number of particles, and the number of sample steps on the statistical error. Hadjiconstantinou et al. [22] also studied the behavior of statistical fluctuations utilizing equilibrium statistical mechanics. They derived a mathematical expression of statistical error for hydrodynamic variables in order to predict the required number of sample steps.

In all previous studies, however, just one type of error (i.e., either decomposition or statistical error) was considered in the analysis while other types of error were neglected by assuming given values for relevant parameters. Moreover, only limited quantities (e.g., transport coefficients and temperature) in simple situations were considered, even though all hydrodynamic variables (e.g., density, velocity, shear stress) are required for full understanding of the behavior of errors. In the present work, in order to overcome these shortcomings, a new verification method based on the exact physical laws of conservation—mass, linear momentum, and total energy—is introduced. *To the best knowledge of the authors, no verification method and consequent convergence analysis of DSMC based on the physical laws of conservation have been reported in the literature*. It must be reiterated that the physical laws of conservation is an *exact* consequence of the Boltzmann equation owing to the property of collisional invariances of mass, momentum, and total energy. Therefore, all the computational methods intended to solve the Boltzmann equation accurately must satisfy in principle the laws of conservation as well.

The verification may be defined as the process of determining that a computational model implementation accurately represents the developer's conceptual (or mathematical) description of the model, and the solution to the model [23]. In the case of verification of computational models of fluid dynamics based on the Navier-Stokes-Fourier equations, there

already exist several well-established practices [23] developed in past decades. These include making sure there is a correct numerical framework, such as *the conservative form of equations, thereby guaranteeing that numerical solutions strictly satisfying the physical laws of conservation*; convergence study with several grids with different cell-sizes; and application of benchmark problems with known exact (analytic) solutions. The DSMC method converges to the Boltzmann equation by directly simulating particles with no need of solving partial differential equations. Nonetheless, the DSMC method is not immune to verification and validation since it is also subject to certain physical laws, the boundary condition, and the post-processing method employed.

A key observation in developing a new verification method for the DSMC method is that the DSMC should satisfy certain physical laws from both macroscopic and microscopic point of views. In the DSMC method, the post-collision particle's properties are calculated in such a way that linear momentum and total energy are preserved during inter-particle collisions. The angular momentum is not conserved in most collision models; however, this does not have a significant effect on non-rotating flows. Therefore, the physical laws are almost satisfied locally in microscopic aspect. However, the local physical laws of conservation in microscopic space do not guarantee the global physical laws of conservation in macroscopic space. In particular, introduction of computational boundary conditions of approximate nature may have a significant effect on the outcomes in macroscopic space. Additionally, the DSMC method is a statistical method in which statistical uncertainty exists at each of the simulation cells and spreads out through the simulation domain. The amount of statistical error also varies among simulation cells due to different sample size at each simulation cell. Moreover, a large number of particles are being used in most DSMC simulations. Therefore, the aggregation of insignificant errors related to the local and global non-conservation may lead

to considerable error in final solutions. Based on this observation, the level of deviation from conservation laws may be used as an indicator of verification for the DSMC method.

In this study, a new verification method based on conservation laws was applied to investigate the behavior of various errors by solving two well-known benchmark problems: the high Mach number shock structure and planar compressible Couette flow problems. The shock structure problem was considered in order to isolate the inherent characteristics of DSMC method from the wall boundary condition effects, while the Couette flow problem was chosen to investigate the effects of numerical wall boundary conditions on the accuracy of the DSMC method in detail. In addition, a convergence history plot was presented with the purpose that it can illustrate the total amount of deviation from conservative laws in each step of the simulation. This convergence history plot is expected to be easily utilized for all kinds of problems, with any spatial dimension and geometry, and for studying the behavior of various errors—decomposition, statistical, machine, and boundary condition—in the DSMC method.

2. New verification method based on conservation laws

The Navier-Stokes-Fourier equations are being used to describe the behavior of Newtonian fluids in a wide spectrum of applications such as aircraft, automotive, petroleum, and turbo machinery. However, this linear continuum approach is no longer valid under rarefied and highly non-equilibrium conditions. In order to describe more accurately the behavior of constitutive molecules in these conditions, fundamental kinetic theory is needed [24]. The gas kinetic theory can provide proper relationships between conserved properties (i.e., velocity, density and temperature) and non-conserved properties (i.e., shear stress and heat flux). These relationships can be based on either particle distribution function or moment equations [25-31].

On the other hand, the DSMC method tries to directly model the physical behavior of gases by simulating the motion of representative particles at microscopic level. However, it must be noted that the final solution of the DSMC method, similar to other methods based on the gas kinetic theory, is macroscopic properties of gases. Therefore, *these macroscopic properties must also satisfy the exact physical laws in a self-consistent way, irrespective of computational models*, which means that the following conservation laws must be satisfied by the DSMC method [32, 33];

$$\frac{\partial \mathbf{U}}{\partial t} + \frac{\partial \boldsymbol{E}}{\partial x} + \frac{\partial \boldsymbol{F}}{\partial y} + \frac{\partial \boldsymbol{G}}{\partial z} = 0, \tag{2.1}$$

where **U** represents the conserved variables, **E**, **F**, and **G** are the fluxes. The components of equation (2.1) are defined as follows:

$$\mathbf{U} = \begin{bmatrix} \rho \\ \rho u \\ \rho v \\ \rho w \\ \rho E \end{bmatrix}$$

$$\boldsymbol{E} = \begin{bmatrix} \rho u \\ \rho u^2 + p - \Pi_{xx} \\ \rho uv - \Pi_{xy} \\ \rho uw - \Pi_{xz} \\ (\rho E + p)u - u\Pi_{xx} - v\Pi_{xy} - w\Pi_{xz} + Q_x \end{bmatrix}$$

$$\boldsymbol{F} = \begin{bmatrix} \rho v \\ \rho uv - \Pi_{xy} \\ \rho v^2 + p - \Pi_{yy} \\ \rho vw - \Pi_{yz} \\ (\rho E + p)v - u\Pi_{xy} - v\Pi_{yy} - w\Pi_{yz} + Q_y \end{bmatrix}$$

$$\boldsymbol{G} = \begin{bmatrix} \rho w \\ \rho uw - \Pi_{xz} \\ \rho vw - \Pi_{yz} \\ \rho w^2 + P - \Pi_{zz} \\ (\rho E + p)w - u\Pi_{xz} - v\Pi_{yz} - w\Pi_{zz} + Q_z \end{bmatrix}$$

where $\rho, u, v, w, p, E, \prod_{ij}, Q_i$, and are density, velocity components, pressure, energy, shear stress tensor, and heat flux vector, respectively. Also, these equations can be written in the form of integral terms which can be more useful for two and three dimensional problems:

$$\frac{\partial}{\partial t} \int_V \mathbf{U} dV + \oint_S \mathbf{F} \cdot \mathbf{n} dS = 0 \qquad (2.2)$$

where S represents the surface bounding around the control volume V.

These forms of conservation laws among the variables $\rho, \mathbf{u}, p, \mathbf{\Pi}, \mathbf{Q}$—including 2D and 3D flow cases—can then be used as a self-consistent method to verify the DSMC method by checking the total amount of errors. In case of the pure one-dimensional steady state flow problem, the conservation laws (2.1) are reduced to the following system of ordinary differential equations:

$$\frac{\partial}{\partial x} \begin{bmatrix} \rho u \\ \rho u^2 + p - \prod_{xx} \\ \rho uv - \prod_{xy} \\ \rho uw - \prod_{xz} \\ (\rho E + p)u - u\prod_{xx} - v\prod_{xy} - w\prod_{xz} + Q_x \end{bmatrix} = \begin{bmatrix} 0 \\ 0 \\ 0 \\ 0 \\ 0 \end{bmatrix} \qquad (2.3)$$

It must be emphasized that these physical conservation laws are *the exact consequence of the kinetic Boltzmann equation,*

$$\frac{\partial f}{\partial t} + \mathbf{v} \cdot \nabla f = C[f, f_2],$$

valid for all degrees of non-equilibrium. Here the term $C[f, f_2]$ represents the Boltzmann collision integral of the interaction among the particles. Only after some approximations like the linear Navier and Fourier (or Chapman-Enskog in kinetic theory terms) constitutive relations, $\mathbf{\Pi} \sim \nabla \mathbf{u}$, $\mathbf{Q} \sim \nabla T$, are introduced for the stress tensor and the heat flux vector, they become approximate, thereby valid only at near-thermal-equilibrium.

The conservation laws (2.3) can be derived directly from the kinetic Boltzmann equation as follows: for example, in the case of momentum conservation law, differentiating the

9

statistical definition of the momentum with time and combining with the Boltzmann equation yield

$$\frac{\partial}{\partial t}\langle m\mathbf{v}f\rangle = \left\langle m\mathbf{v}\frac{\partial f}{\partial t}\right\rangle = -\langle m(\mathbf{v}\cdot\nabla f)\mathbf{v}\rangle + \langle m\mathbf{v}C[f, f_2]\rangle.$$

Then the first term on the right-hand side becomes

$$-\langle m(\mathbf{v}\cdot\nabla f)\mathbf{v}\rangle = -\nabla\cdot\langle m\mathbf{v}\mathbf{v}f\rangle = -\nabla\cdot\{\rho\mathbf{u}\mathbf{u} + \langle m\mathbf{c}\mathbf{c}f\rangle\}.$$

The symbols $\mathbf{v}, \mathbf{c}, \mathbf{u}, \langle\ \rangle$ denote the particle velocity, the peculiar velocity, the average bulk velocity, and the integral in velocity space, respectively. After the decomposition of the stress $\mathbf{P}$ into the pressure p and the viscous stress $\mathbf{\Pi}$ ($[\ \ ]^{(2)}$ denoting the traceless symmetric part of the tensor),

$$\mathbf{P} \equiv \langle m\mathbf{c}\mathbf{c}f\rangle = p\mathbf{I} - \mathbf{\Pi} \text{ where } p \equiv \langle m\text{Tr}(\mathbf{c}\mathbf{c})f/3\rangle, \ \mathbf{\Pi} \equiv -\langle m[\mathbf{c}\mathbf{c}]^{(2)}f\rangle,$$

and using the collisional invariance of the momentum, $\langle m\mathbf{v}C[f, f_2]\rangle = 0$, we obtain

$$\frac{\partial(\rho\mathbf{u})}{\partial t} + \nabla\cdot(\rho\mathbf{u}\mathbf{u} + p\mathbf{I} - \mathbf{\Pi}) = 0,$$

an exact consequence of the original kinetic Boltzmann equation. A similar method with the statistical definition of the heat flux, $\mathbf{Q} \equiv \langle mc^2\mathbf{c}f/2\rangle$, can be applied to the derivation of the energy conservation law. Note that the equation (2.3) is nothing but the one-dimensional steady-state version of the conservation laws. For this reason, the exact physical conservation laws (2.3) to the Boltzmann equation will be utilized for studying two benchmark problems in the next section.

2.1. Shock structure problem

The stationary shock wave structure is a pure one-dimensional compressive gas flow defined as a very thin (order of mean free path) stationary gas flow region between the supersonic upstream and subsonic downstream [34]. The shock wave structure is one of the

most-studied problems in gas dynamics, since it is not only important from the technological viewpoint, but it has also been a major stumbling block for theoreticians for a long time [35-40]. In addition, the wall boundary condition is not present in this one-dimensional problem so that one may study the inherent behavior of a numerical method free from the contamination caused by the solid wall boundary condition.

In the case of the shock wave structure problem, the one-dimensional conservation laws (2.3) are reduced as follows: still exact to the original Boltzmann equation,

$$
\frac{\partial}{\partial x}
\begin{bmatrix}
\rho u \\
\rho u^2 + p - \Pi_{xx} \\
-\Pi_{xy} \\
-\Pi_{xz} \\
(\rho E + p)u - \Pi_{xx}u + Q_x
\end{bmatrix}
= 0 \implies
\begin{aligned}
\rho u &= C_1 \\
\rho u^2 + p - \Pi_{xx} &= C_2 \\
-\Pi_{xy} &= C_3 \\
-\Pi_{xz} &= C_4 \\
(\rho E + p)u - \Pi_{xx}u + Q_x &= C_5
\end{aligned}
\tag{2.4}
$$

Then, the errors associated with the conservation laws may be defined at each point of simulation domain as:

$$
\begin{aligned}
\text{error}_{mass} &\equiv \rho u - \overline{\rho u} \\
\text{error}_{x-momentum} &\equiv \rho u^2 + p - \Pi_{xx} - \left\{ \overline{\rho u^2 + p - \Pi_{xx}} \right\} \\
\text{error}_{y-momentum} &\equiv -\Pi_{xy} + \overline{\Pi_{xy}} \\
\text{error}_{z-momentum} &\equiv -\Pi_{xz} + \overline{\Pi_{xz}} \\
\text{error}_{energy} &\equiv (\rho E + p)u - \Pi_{xx}u + Q_x - \left\{ \overline{(\rho E + p)u - \Pi_{xx}u + Q_x} \right\} \\
\text{error}_{EOS} &\equiv p - \rho R T \qquad \implies \text{Round-off error}
\end{aligned}
\tag{2.5}
$$

where the symbol $\bar{\square}$ denotes representatives reference values of conservative values $\square$ and they can be taken as either average values of macroscopic properties in the whole domain, or as the upstream values. In this study, the $\bar{\square}$ values are calculated based on the average values of macroscopic properties in the whole domain, which should be distinguished from the cumulative averaging method commonly used in the sampling procedure of the DSMC method.

11

2.2. Compressible Couette flow problem

The Couette flow is defined as the flow trapped between two infinite, parallel, flat plates at $x = \pm H$ driven by the shear motion of one or both of the plates in opposite directions with constant velocity, while the temperature of the walls is constant. It is also assumed that the fluid moves in the *y*-direction only, as shown in Fig. 2. The flow is considered to be steady state, one-dimensional, compressible and without any external forces. Therefore, this shear-driven flow problem is an excellent benchmark case for studying the effects of the solid wall boundary condition on the accuracy of the DSMC method. In the case of the Couette flow problem, the one-dimensional conservation laws (2.3) are reduced: still exact to the original Boltzmann equation,

$$\frac{\partial}{\partial x}\begin{bmatrix} 0 \\ p - \Pi_{xx} \\ -\Pi_{xy} \\ -\Pi_{xz} \\ -\Pi_{xy}v + Q_x \end{bmatrix} = 0 \quad \Rightarrow \quad \begin{matrix} p - \Pi_{xx} = C_1^{'} \\ -\Pi_{xy} = C_2^{'} \\ -\Pi_{xz} = C_3^{'} \\ -\Pi_{xy}v + Q_x = C_4^{'} \end{matrix} \tag{2.6}$$

The errors associated with the conservation laws are then defined as follows:

$$
\begin{aligned}
&\text{error}_{x-momentum} \equiv p - \Pi_{xx} - \left[\overline{P - \Pi_{xx}} \right] \\
&\text{error}_{y-momentum} \equiv \Pi_{xy} - \overline{\Pi_{xy}} \\
&\text{error}_{z-momentum} \equiv \Pi_{xz} - \overline{\Pi_{xz}} \\
&\text{error}_{energy} \equiv -\Pi_{xy}v + Q_x - \left[\overline{-\Pi_{xy}v + Q_x} \right] \\
&\text{error}_{EOS} \equiv p - \rho RT \quad \Rightarrow \quad \text{Round-off error}
\end{aligned}
\tag{2.7}
$$

where C_i and $C_i^{'}$ are integration constants called conservative values in the following sections since they remain constant throughout the simulation domain.

3. Results and discussion

3.1. Verification of DSMC

In order to verify the direct simulation Monte Carlo method, hard sphere gas molecule was used. The values of time-step and cell-size were chosen extremely small, while the mean

number of particles in each cell was selected large enough to minimize the simulation error. In addition, the sampling procedure was being continued until the statistical fluctuation became negligible. Moreover, the references mean collision time, τ_∞, and mean free path, λ_∞, were calculated based the hard sphere relationship [3] and the free stream macroscopic properties, respectively.

3.1.1. Shock structure problem

According to the conservation laws (2.4), the values of mass, momentum and total energy should be constant throughout the simulation domain. In order to investigate the accuracy of the DSMC method in detail, deviations from conservation laws were measured throughout the domain based on equation (2.5) for a representative monatomic gas (molecular diameter 4×10^{-10} meter and molecular mass 6.64×10^{-26} kg). The upstream Mach number is set to be two, and a stabilizer [3] was used to fix the location of the stationary shock. The two and infinity norms of error were calculated to monitor the total error values for each test case. Figure 3 shows that the absolute and relative errors associated with conservation laws (notably, mass, x-momentum, y-momentum, z-momentum, and total energy), remained mostly constant throughout the domain. Interestingly, a small hike in the error of x-momentum conservation is found at the center of the shock structure, as highlighted by a square box in Fig. 3, while there is no such abnormality in other errors. This spike in the x-momentum error may be related to insufficient collisions between particles to maintain local equilibrium in the shock region since the macroscopic properties vary in the scale of local mean free path. In addition, the shear stress—second order moments of the distribution function—is rapidly increasing inside the shock region, leading to the high degree of non-equilibrium and decrease of the local mean collision time and ultimately higher x-momentum error. Hence, in order to reduce computational errors in this region, proper cell-size and, in particular, small time-step size may be required.

Figure 3 also indicates that, due to different units in the conservation equations, the error produced by the energy equation seems considerably high, in comparison with other equations. However, the relative error, free from this unit gap, may be more convenient for examining the behavior of errors in detail. The results show that the relative errors are very small in case of the shock structure problem for all conservation laws (in the case of L_2 norm, 5.0397×10^{-5}, 1.1544×10^{-4}, 1.5637×10^{-4}, for mass, x-momentum, and energy, respectively).

Thus, the present DSMC results obtained for the proper ranges of time-step, cell-size, number of particles per cell, and the number of sample steps ($\Delta t = 0.01\tau_\infty$, $\Delta x = 1/32\lambda_\infty$, $N = 320$, $N_S = 10^8$) can be considered as a correct solution, in the sense that they satisfy the physical laws of conservation with a very high level of accuracy. This outcome may be regarded as a computational proof of the DSMC method, similar to a mathematical proof derived by Wagner [12]. Round-off error represented by the equation of state is also reported to quantify the maximum limit of precision in the simulation.

3.1.2. Compressible Couette flow problem

In order to investigate the effect of the gas-surface molecular interaction, on the accuracy of the DSMC method, the Couette flow driven by shear motion was considered. In the Couette flow simulation, two diffuse walls having constant temperature (293 K) are moving in opposite directions with constant velocity corresponding to Mach number 1 (relative Mach number two). The same monatomic gas properties used in the simulation of the shock structure problem were applied here. The Knudsen number based on the gap between walls was assumed to be 1.0. The values of $\Delta t = 0.01\tau_\infty$, $\Delta x = 1/32\lambda_\infty$, $N = 320$, $N_S = 10^8$ were used for time-step, cell-size, number of particles per cell, and the number of sample steps, respectively. The conservative values, calculated using equation (2.6), are depicted in Fig. 4. As explained previously, these values should be constant throughout the simulation domain

in order that conservation laws may be satisfied in the simulation. Figure 4 shows that the conservative values were almost constant everywhere in the computational domain, except in the cells near the wall. To further investigate, absolute and relative errors were calculated based on equation (2.7) and their values are shown in Fig. 5. The results indicate several things. First, they show that there exist errors arising from wall boundary condition. Second, that the errors produced by the y-momentum and energy equations are relatively high, and third, that the errors in energy and y-momentum equations increase near the wall (as high as two orders of magnitude) in comparison with the bulk flow region. However, the exact cause of these deviations from conservation laws appearing coupled with decomposition errors in the simulation is not yet known, implying that further investigations are needed to obtain a definite conclusion.

3.2. Viscosity index effect

The effect of different values of viscosity index (ω) on the error of conservation laws was also investigated by solving the shock structure problem. The absolute and relative errors are depicted in Fig. 6, for x-momentum and energy equations. The results show that the magnitude of error remains almost the same for all viscosity indices ω. The error in x-momentum equation is more sensitive to the viscosity index, in particular, in domain of steep spatial gradient within the shock structure, while the error in energy equation does not show such behavior for all viscosity indices. Therefore, it may be better to measure error in x-momentum to analyze the effect of the viscosity index on the accuracy of the DSMC method. Furthermore, the amount of error in x-momentum equation decreases with increasing viscosity index. As a result, the Maxwellian and hard sphere gas molecules showed the lowest and highest levels of deviation from conservation laws, respectively. Nonetheless, the absolute value of deviations remained small for all viscosity indices. This finding coincides

15

with the study of Torczynski et al. [41] in which the Sonine polynomial coefficients of Chapman-Enskog theory for heat flux were compared with DSMC results.

3.3. Convergence analysis

The CFD methods based on deterministic partial differential equations can naturally report the run-time residual to examine the stability and error behaviors of the numerical method. However, it is not obvious how to report such convergence history in the case of the DSMC method. The DSMC method itself is computationally efficient and very robust, in the sense that it never exhibits instability during simulation. Therefore there is less interest in reporting the convergence history plot to check instability. However, measuring and reporting the amount of error at every simulation step remains crucial, even in the DSMC method.

The DSMC method is a statistical approach which directly simulates the physics, instead of solving partial differential equations. Consequently, it is not an easy task to define a convergence history plot for a DSMC simulation. The convergence history plot should be able to describe the contribution of various error sources when the simulation is running. Only a small amount of research has been conducted to predict the number of sample steps required to minimize the statistical noise and fluctuations in the DSMC method[22]. However, these studies only estimated the value of statistical error (based on equilibrium statistical mechanics) among four types of error, and did not consider the others.

In the present study, a convergence history based on the physical laws of conservation was introduced for analyzing convergence behavior of the DSMC during a simulation run. Even though a one-dimensional problem was considered here for the sake of simplicity, it can easily be extended to multi-dimensional flow problems. The method is expected to describe the inherent characteristics of physical and statistical behavior of the DSMC method.

Statistical methods like DSMC employ a sampling procedure to reduce statistical noise, and to obtain population (or macroscopic) properties. The standard error of the mean (SEM),

which describes the standard deviation of the error in the sample mean relative to the population mean, can be reduced by increasing the sample size. The SEM is a function of the inverse square root of the sample size (the number of particles and the number of sample steps) in the DSMC method. In addition, it is known that each hydrodynamic variable shows unique behavior in statistical error [22]. Thus, the combination of these variables may lead to unique statistical behavior. As a result, the convergence behavior will be different for each of the conservation equations, since different conservation equations involve different combinations of hydrodynamic variables. In the following sections, results are presented of tests on the new method, for various conditions used to analyze the behavior of convergence.

3.3.1. Number of sample steps

The influence of the number of sample steps on convergence is presented first. Figures 7 and 8 illustrate the convergence history of a DSMC simulation of compressible Couette flow ($M = 2.0$, Kn=1.0 , $\Delta t = 0.01\tau_\infty$, $\Delta x = 1/32\lambda_\infty$, $N = 320$). The two and infinity norms of errors were calculated for all conservation equations at each simulation step. The convergence behavior seems to be composed of two separate phases. In the first phase, statistical error is dominant. This phase continues until the number of sample steps reaches certain values, so that the contribution of the statistical error to total error becomes negligible. The results also show that, as expected, the total error in the first phase decreased with increasing the number of sample steps. Furthermore, the rate of this decrease is inversely proportional to the square root of the sample steps ($1/\sqrt{N_s}$). The second phase starts when the combination of boundary condition and decomposition errors becomes prominent, in comparison with statistical error. The decomposition and boundary condition errors do not decrease with increasing sample size, since these errors do not depend on sample steps. The decomposition error can be changed by adjusting the physical parameters like time-step interval size.

3.3.2. Number of particles

The number of particles is another important factor in statistical error. It is directly proportional to the sample size and thus can influence the rate of convergence as the number of sample steps does [3, 42]. The decrease of statistical error is proportional to $1/\sqrt{mN}$, where m is a constant value multiplied by the initial number of particles N. In order to check the capability of the present method to capture this statistical feature, several simulations with different numbers of particles were conducted for problems in which ($M = 2.0$, Kn=1.0, $\Delta t = 0.01\tau_\infty$, $\Delta x = 1/32\lambda_\infty$, $N_S = 10^8$). Figure 9 shows the convergence history for x-momentum and energy conservation equations. Here, statistical error is shown to play a dominant role compared to other types of error. The results also show the convergence rates for various cases with different number of particles. The solid line represents the test case with an average of 40 particles in each cell. The solid lines with circular, triangular and diamond symbols represent test cases with approximately 80, 160, 320 particles per cell, respectively. The simulation with approximately 40 particles per cell was used as a reference, and dotted lines drawn based on the relation between the number of particles and the SEM value, $1/\sqrt{mN}$. These dotted lines represent the theoretical statistical convergence rate for the DSMC method when different numbers of particles are used in the simulation. Overall, the results show that the present method can properly describe the effect of different numbers of particles on convergence.

In Figs. 10 and 11, the convergence history is also plotted for cases with larger sample steps. The results show that the total error decreases quickly with increasing sample size, but does not vanish completely. Owing to the presence of the decomposition and boundary condition errors, the total error converges to a finite constant value, even when an infinite number of samples, or particles, is used. In other words, more particles can result in a faster

convergence rate for the statistical part, but this does not change the decomposition and boundary condition errors.

The round-off error may also be observed by examining error values for the equation of state in Fig. 11. The values show the maximum limit of accuracy of the current simulation, and that it is not changed by increasing sample steps or number of particles. Moreover, the statistical error in the z-momentum equation does not converge to any constant value; it still declines, even after more than 10^8 samples. A possible explanation for this behavior is that the z spatial direction does not exist in the present 1D-Coutte flow problem. Particles are not moving and colliding in the z spatial coordinate, so that the convergence rate of z-momentum error will follow the statistical error pattern and flatten after reaching to the limit of round-off error limit.

3.4. Computational parameters associated with decomposition error

Computational parameters associated with decomposition error—time-step interval size, cell-length size, and number of particles—can influence the accuracy of the DSMC method significantly. In this section, the use of the physical laws of conservation is applied in order to check the accuracy of the DSMC method for various computational parameters. It is expected that the present study could be useful to find a proper value for computational parameters such that conservation laws are satisfied by the DSMC in acceptable level. The shock structure problem with the upstream Mach number 2.0 was chosen in order to avoid excessive error from the wall boundary condition. Several simulations with different time-step interval sizes, cell-length sizes and numbers of particles were considered.

3.4.1. Time-step

The time-step size, Δt, is one of the most important computational parameters that can affect the decomposition error. This computational parameter plays a critical role in decoupling the movement and collision steps in the DSMC method. The errors measured

based on deviations from conservation laws, with $\Delta x = 1/32\lambda_\infty$, $N = 320$, $N_S = 10^8$, are shown

in Fig. 12. It can be observed that the error decreased as the time-step size decreased. Also,

the errors in three important conservation equations—mass, x-momentum, and energy—

became noticeable for larger values of time-step. The figure also illustrates that, as expected,

the round off error does not depend on the time-step value.

Figure 13 shows the shock structure profiles of density, velocity, normal stress, and heat

flux for cases with different values of Δt. These results illustrate that the non-conserved

normal stress, and the heat flux, variables are more sensitive to the time-step compared to

other conserved variables. The simulation solutions with larger time-steps led to overly

smoothed profiles of normal stress and heat flux, probably due to excessively larger

numerical viscosity than to actual physical viscosity caused by the larger time-step. Since the

non-conserved normal stress and the heat flux are directly related to spatial gradients in the

flow field, it would be instructive to compare the effect of the time-step on the gradients of

the hydrodynamic variables. Figure 14 depicts the velocity gradient versus the density

gradient for four different test cases. The gradients increased dramatically as the time-step

decreased, then reached asymptotic value, meaning that an accurate solution free from the

decomposition error of time-step may be obtained.

Finally, the relative errors were calculated for four different time-steps, as shown in Fig.

15. This shows that the error is much greater in the momentum conservation equation than in

the other conservation equations for all Δt. In addition, the relative x-momentum error

reaches as high as 5% at $\Delta t = \tau_\infty$ and falls drastically to reach 0.6% at $\Delta t = 0.1\,\tau_\infty$ before

declining slightly afterward. This means that the error of the DSMC method can be

significantly reduced by using a smaller time-step value. Also, the conservation of x-

momentum is more sensitive to time-step in comparison with the conservation of energy and

mass; at least for the present Mach number, cell-size, and number of particles.

3.4.2. Cell length size

The cell-size Δx is another important computational parameter that can influence the decomposition error. Here different cell-sizes are considered in order to study the effect of cell-size on the behavior of error in the DSMC method. All other computational parameters were selected properly so that the effect of cell size may be pronounced ($\Delta t = 0.01\tau_\infty$, $N = 320$, $N_S = 10^8$). The shock structure profiles of density, velocity, normal stress, and heat flux for six cases with different cell-sizes are plotted in Fig. 16. The results show that difference in cell-size does not yield much difference in the profiles, including normal stress and heat flux, which is in contrast with the previous case of varying the time step. This means that the error of the DSMC method is sensitive to both of the time-step and the cell-size. Also, the resolution of simulation results increases linearly as the cell size decreases. Figure 17 depicts the velocity gradient versus the density gradient for six cases with different cell-size. The bigger cell-size led to smaller gradients, probably due to larger numerical viscosity involved during the simulation. The gradients of hydrodynamic variables did not change significantly when the cell-size is smaller than $0.125\lambda_\infty$, where λ_∞ was the mean free path of the free stream. As a result, cell-size may be selected in such a way that the simulation outcomes are not changed by reducing the cell-size.

Figure 18 shows the relative errors when Δx changes from λ_∞ to $\lambda_\infty/32$. It can be seen that the error in the x-momentum conservation equation is much higher than those of other two conservation equations for all Δx. Also, the amount of error for the x-momentum equation, initially 0.07% at $\Delta x = \lambda_\infty$, decreased slightly to reach 0.057% at $\Delta x = \lambda_0/8$, followed by a dramatic drop at $\Delta x = \lambda_0/16$ and flattening-off afterward. However, the error of the mass conservation equation showed a slight decrease before dropping sharply at $\Delta x = \lambda_\infty/2$ and then decreasing gradually to reach a minimum value of 0.012% at

$\Delta x = \lambda_\infty / 32$. On the other hand, the error of the energy conservation equation decreased moderately to reach a minimum value of 0.008% at $\Delta x = \lambda_\infty / 32$. Overall, it was found that the momentum conservation equation is more sensitive to the size of the cells than were the other conservation equations. The bigger cells, as expected, produced greater error, but the amount of error remained negligible for all cases considered.

3.4.3. Number of particles

The last computational parameter associated with decomposition error is the number of particles, N, in simulation domain. Several test cases with different numbers of particles per cell (and with $\Delta t = 0.01\tau_\infty$, $\Delta x = 1/32\lambda_\infty$, $N_S = 10^8$) were considered to examine the effect of number of particles on decomposition error, and on the convergence behavior of the DSMC method. The shock structure profiles of the hydrodynamic variables and their gradients are shown in Figs. 19 and 20. These show that different numbers of particles does not yield much difference in the profiles, including normal stress and heat flux, which is similar to the previous case of varying the cell-size. However, comparison of velocity and density gradients demonstrated a non-negligible difference among cases with 5 and 20 particles per cell.

Figure 21 shows the relative error when the number of particles per cell changes from $N=5$ to $N=1,280$. It can be seen that the error of the x-momentum conservation equation is in general much greater than that of the other two conservation equations. Also, as the number of particles increased from $N=5$ to $N=40$, the errors decreased drastically and then flattened off, implying the existence of an asymptotic value. Overall, similar to the previous case of varying the cell-size, the momentum conservation equation is more sensitive to the number of particles compared to other conservation equations, and the amount of error remains negligible for all cases considered.

4. Summary and concluding remarks

Verification and validation become critical practical issues when laboratory level research of computational models is used in the mature, real world (application) problems. However, such study is often both complicated and subtle since verification and validation of computational models depend on the properties considered and, in many cases, overall multi-faceted agreement is very difficult to achieve. For example, the CFD dispersion of lift in aerodynamics is already within the goal dispersion, whereas the CFD dispersion of drag is far from the goal dispersion.

The primary goal of the present study was to present a new method as a step toward developing a verification tool for pure simulation methods like the DSMC. Though other studies have been devoted to this issue from both mathematical and computational viewpoints in the past, there remain unsolved problems regarding verification of the DSMC method, as it is difficult to find exact solutions free from computational errors—essential in the verification study—for the DSMC method. For the VHS collision model, the conventional Bird's algorithm based on NTC (no time counter) was employed in the present study for its simplicity. For other collision models, the results of error characteristics may be different, but we believe that the essence of the present study will remain unchanged since the errors based on the laws of conservation—exact consequence of the Boltzmann equation—can be defined universally, irrespective of the details of collision model.

Furthermore, most of the previous research was directed to the study of the role of computational parameters on only one type of error, (i.e. either decomposition error or statistical error), while other types of error were ignored. In this study, the exact physical laws of conservation were utilized as a new verification tool to measure the errors in the DSMC method.

Results from the present study show that the error level of the DSMC method is negligible when the critical computational parameters—time-step, cell-size, number of particles—selected in the simulation are well within the asymptotic range. This finding agrees with the results obtained theoretically by Wagner. However, the study of compressible Couette flow driven by shear motion of the solid walls with isothermal and fully diffusive wall conditions seems to indicate that there exist small deviations arising from wall surface boundary conditions. The exact cause of these deviations appearing coupled with decomposition errors in the simulation is not yet known; it may be due to the approximate nature of the gas-surface molecular interaction models or not-perfect boundary treatment in the DSMC code. This makes essential the further investigation of wall surface boundary condition and its computational implementation in the future.

Furthermore, a convergence history according to the new verification method is proposed for the DSMC method. Such a convergence history can provide information about the amount of deviation from conservation laws that occurs in a DSMC simulation, while all four types of error are present. Convergence behavior, with regard to simulation iterations in the DSMC simulation, can be categorized into two distinct phases. In the first phase, statistical error is dominant and the rate of its decrease is inversely proportional to the square root of the sample steps. In the second phase, the combination of boundary condition and decomposition errors becomes prominent, in compared with the statistical error. Also, the convergence history plot shows that the statistical error shows unique behavior for each of the conservation equations. The results also show that the total error decreases quickly with increasing sample size, but does not vanish. This is because decomposition and boundary condition errors always exist in the simulation domain.

Finally, the effect of computational parameters associated with decomposition error on the accuracy of DSMC was investigated using a variety of test-case simulation. The relative

error measured on the basis of the deviation from conservation laws is sensitive to the time-step, the cell-size, and number of particles. It was also found that the error decreases rather quickly in the initial stage with decreasing time-step and the cell-size and with increasing number of particles before it finally flattens off, implying the existence of an asymptotic value.

5. Acknowledgments

References

[1] C. Shen, Rarefied Das Dynamics: Fundamentals, Simulations and Micro Flows, Springer, 2005.

[2] G.A. Bird, Molecular Gas Dynamics, Clarendon, 1976.

[3] G.A. Bird, Molecular Gas Dynamics and the Direct Simulation of Gas Flows, Oxford Science, 1994.

[4] G.A. Bird, The DSMC Method, CreateSpace, 2013.

[5] C. Sheng, X. Shen, Modelling of acoustic agglomeration processes using the direct simulation Monte Carlo method, J. Aerosol Sci. 37 (2006) 16-36.

[6] M. Wang, Z. Li, Gas mixing in microchannels using the direct simulation Monte Carlo method, Int. J. Heat Mass Transf. 49 (2006) 1696-1702.

[7] J.S. Wu, K.C. Tseng, Analysis of micro-scale gas flows with pressure boundaries using direct simulation Monte Carlo method, Comput. Fluids 30 (2001) 711-735.

[8] F.J. Alexander, A.L. Garcia, B.J. Alder, Direct simulation Monte Carlo for thin-film bearings, Phys. Fluids 6 (1994) 3854-3860.

[9] M. Darbandi, A. Karchani, G. Schneider, The study of rarefied gas flow through microfilters with different openings using MONIR-DSMC, ICNMM2011-ASME (2011) 215-221.

[10] J.S. Wu, F. Lee, S.C. Wong, Pressure boundary treatment in micromechanical devices using the direct simulation Monte Carlo method, JSME Int. J. Series B 44 (2001) 439-450.

[11] D.J. Rader, M.A. Gallis, J.R. Torczynski, W. Wagner, Direct simulation Monte Carlo convergence behavior of the hard-sphere-gas thermal conductivity for Fourier heat flow, Physi. Fluids 18 (2006).

[12] W. Wagner, A convergence proof for Bird's direct simulation Monte Carlo method for the Boltzmann equation, J. Stat. Phys. 66 (1992) 1011-1044.

[13] C. Cercignani, The Boltzmann Equation and its Applications, Springer-Verlag, New York, 1988.

[14] C. Villani, A review of mathematical topics in collisional kinetic theory, Handbook of Mathematical Fluid Dynamics Volume 1, Edited by S. Friedlander and D. Serre, 2002.

[15] E. Meiburg, Comparison of the molecular dynamics method and the direct simulation Monte Carlo technique for flows around simple geometries, Phys. Fluids 29 (1986) 3107.

[16] F.J. Alexander, A.L. Garcia, B.J. Alder, Cell size dependence of transport coefficients in stochastic particle algorithms, Phys. Fluids 10 (1998) 1540-1542.

[17] N.G. Hadjiconstantinou, Analysis of discretization in the direct simulation Monte Carlo, Phys. Fluids 12 (2000) 2634-2638.

[18] A.L. Garcia, W. Wagner, Time step truncation error in direct simulation Monte Carlo, Phys. Fluids 12 (2000) 2621-2633.

[19] D. Rader, M. Gallis, J. Torczynski, W. Wagner, DSMC convergence behavior for Fourier flow, AIP Conference Proceed. (2005).

[20] G. Chen, I.D. Boyd, Statistical error analysis for the direct simulation Monte Carlo technique, J. Comput. Phys. 126 (1996) 434-448.

[21] M.M. Mansour, A.L. Garcia, G.C. Lie, E. Clementi, Fluctuating hydrodynamics in a dilute gas, Phys. Rev. Lett. 58 (1987) 874-877.

[22] N.G. Hadjiconstantinou, A.L. Garcia, M.Z. Bazant, G. He, Statistical error in particle simulations of hydrodynamic phenomena, J. Comput. Phys.187 (2003) 274-297.

[23] W.L. Oberkampf, C.J. Roy, Verification and Validation in Scientific Computing, Cambridge University Press, 2010.

[24] W.G. Vincenti, C.H. Kruger, Introduction to Physical Gas Dynamics, Wiley, 1965.

[25] H. Grad, On the kinetic theory of rarefied gases, Commun. Pure Appl. Math. 2 (1949) 331-407.

[26] B.C. Eu, Kinetic Theory and Irreversible Thermodynamics, Wiley, 1992.

[27] R.S. Myong, A computational method for Eu's generalized hydrodynamic equations of rarefied and microscale gasdynamics, J. Comput. Phys.168 (2001) 47-72.

[28] R.S. Myong, A generalized hydrodynamic computational model for rarefied and microscale diatomic gas flows, J. Comput. Phys.195 (2004) 655-676.

[29] N.T.P. Le, H. Xiao, R.S. Myong, A triangular discontinuous Galerkin method for non-Newtonian implicit constitutive models of rarefied and microscale gases, J. Comput. Phys. 273 (2014) 160-184.

[30] H. Xiao, R.S. Myong, Computational simulations of microscale shock-vortex interaction using a mixed discontinuous Galerkin method, Comput. Fluids 105 (2014) 179-193.

[31] S. Chapman, T.G. Cowling, The Mathematical Theory of Non-uniform Gases: An Account of the Kinetic Theory of Viscosity, Thermal Conduction and Diffusion in Gases, Cambridge University Press, 1970.

[32] R.S. Myong, Impact of computational physics on multi-scale CFD and related numerical algorithms, Comput. Fluids 45 (2011) 64-69.

[33] R.S. Myong, J. Park, Confirmation of non-classical laws in nonequilibrium gases and application of conservation laws to verification of DSMC, AIP Conference Proc. 1501 (2012) 621-628.

[34] T.I. Gombosi, Gaskinetic Theory, Cambridge University Press, 1994.

[35] M. Morduchow, On a complete solution of the one-dimensional flow equations of a viscous, heat-conducting, compressible gas, J. Aeronau. Sci. 16 (2012) 674-684, 704.

[36] H. Mott-Smith, The solution of the Boltzmann equation for a shock wave, Phys. Rev. 82 (1951) 885-892.

[37] H. Grad, The profile of a steady plane shock wave, Commun. Pure Appl. Math. 5 (1952) 257-300.

[38] M. Al-Ghoul, B.C. Eu, Generalized hydrodynamics and shock waves, Phys. Rev. E 56 (1997) 2981-2992.

[39] R.S. Myong, Thermodynamically consistent hydrodynamic computational models for high-Knudsen-number gas flows, Phys. Fluids 11 (1999) 2788-2802.

[40] R.S. Myong, Analytical solutions of the shock structure thickness and asymmetry in the Navier-Stokes-Fourier framework, AIAA J. 52-5 (2014) 1075-1080.

[41] J. Torczynski, M. Gallis, D. Rader, DSMC Simulations of Fourier and Couette flow: Chapman-Enskog behavior and departures therefrom, AIP Conference Proceed. (2005) 620.

[42] A.D. Hanford, Numerical Simulations of Acoustics Problems Using the Direct Simulation Monte Carlo Method, Ph.D. Thesis, ProQuest, 2008.
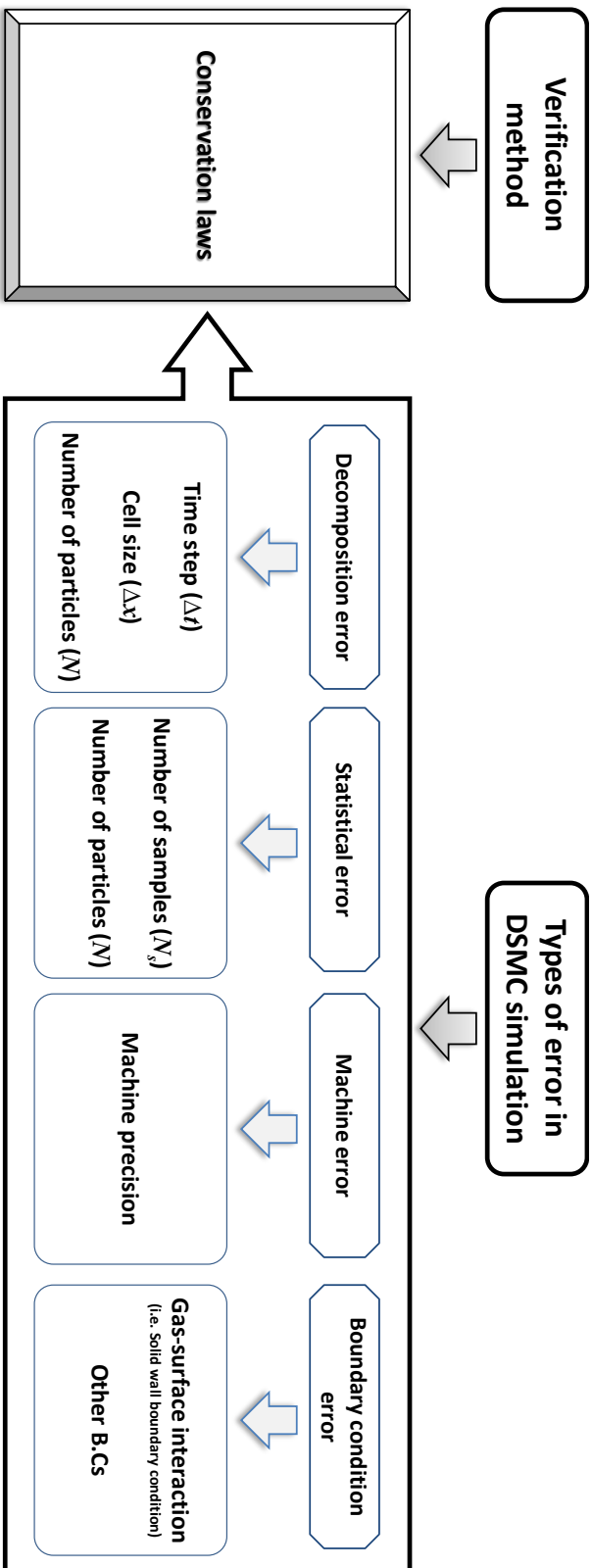
Fig. 1. Types of errors in the DSMC simulation.
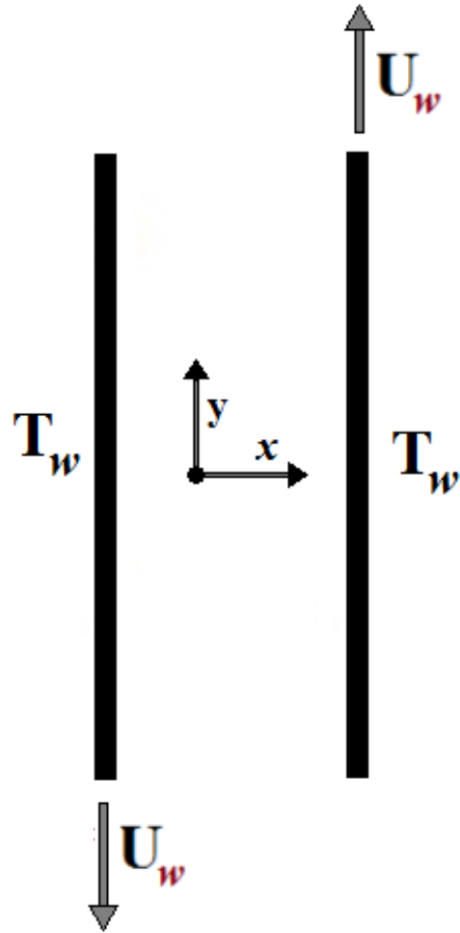
Fig. 2. The schematic of the shear-driven Couette flow.
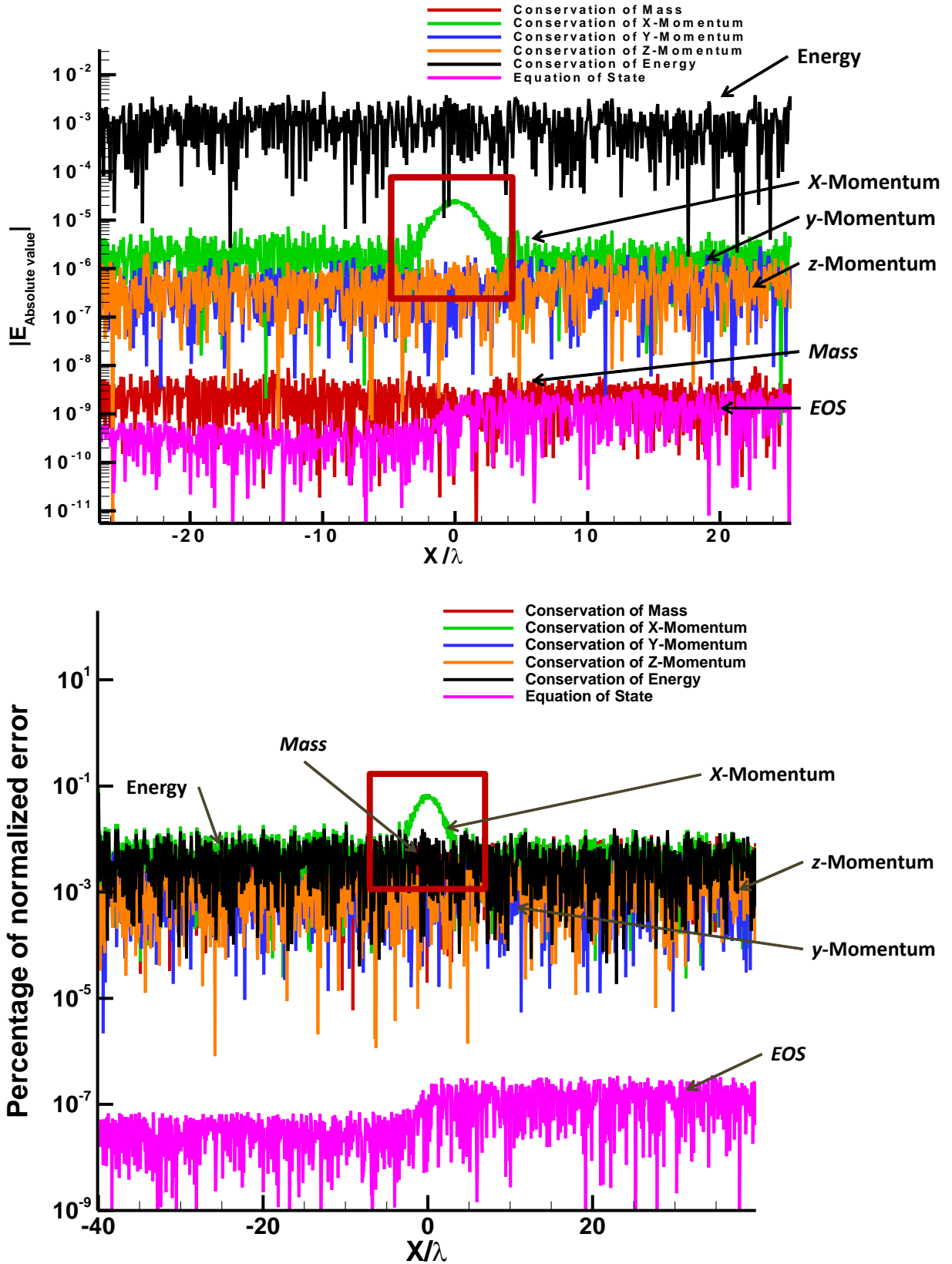
Fig. 3. Absolute (top) and normalized (bottom) errors of all conservation equations in the shock structure problem. The horizontal axis represents *x* spatial coordinate. (Absolute values in the order of energy, *x,z,y*-momentum, mass, EOS, while normalized values in the order of *x*-momentum, energy, mass, *z,y*-momentum, EOS).
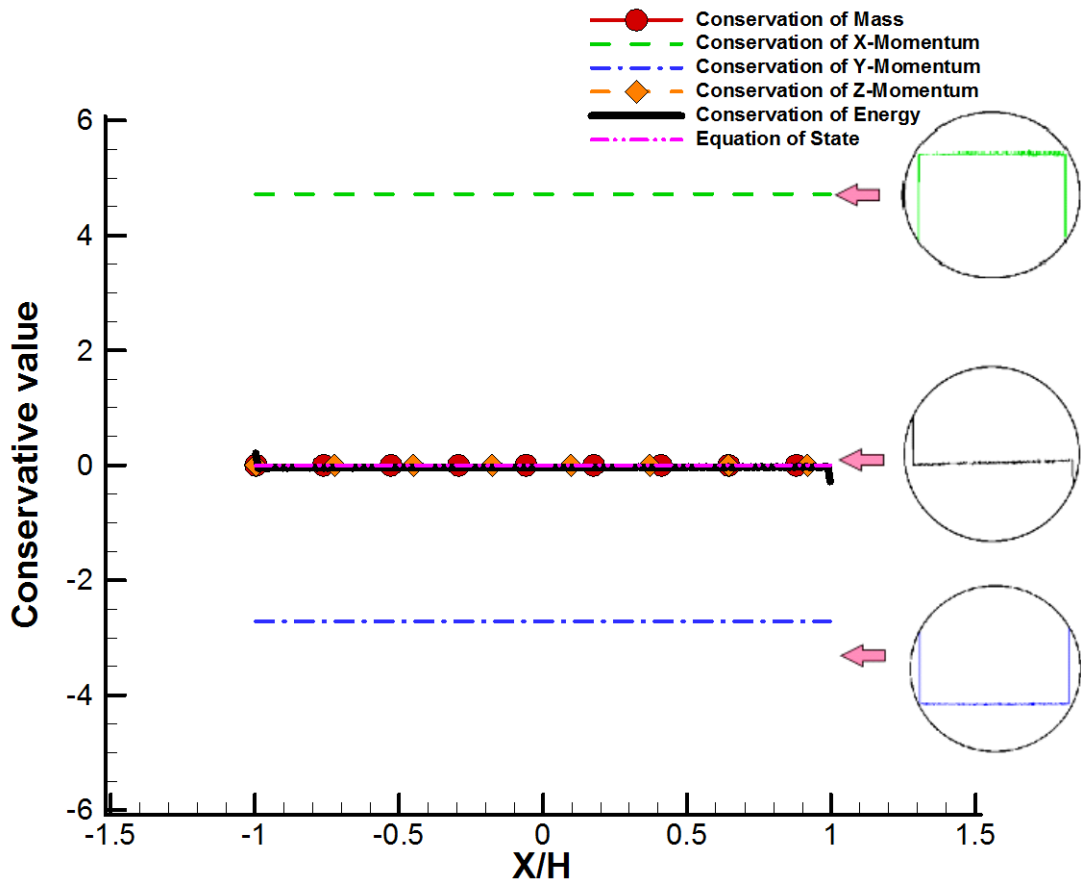
Fig. 4. The conservative values of all conservation equations and equation of state in the compressible Couette flow problem.
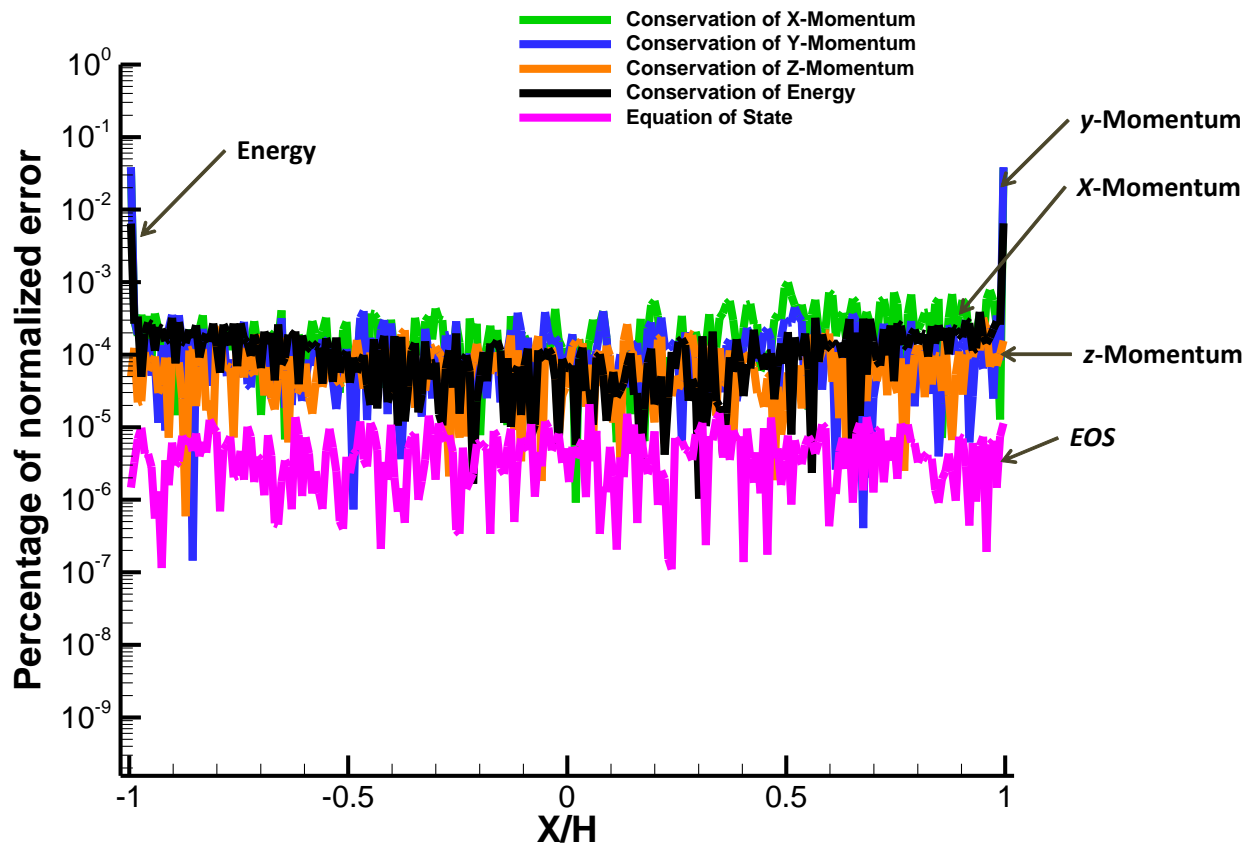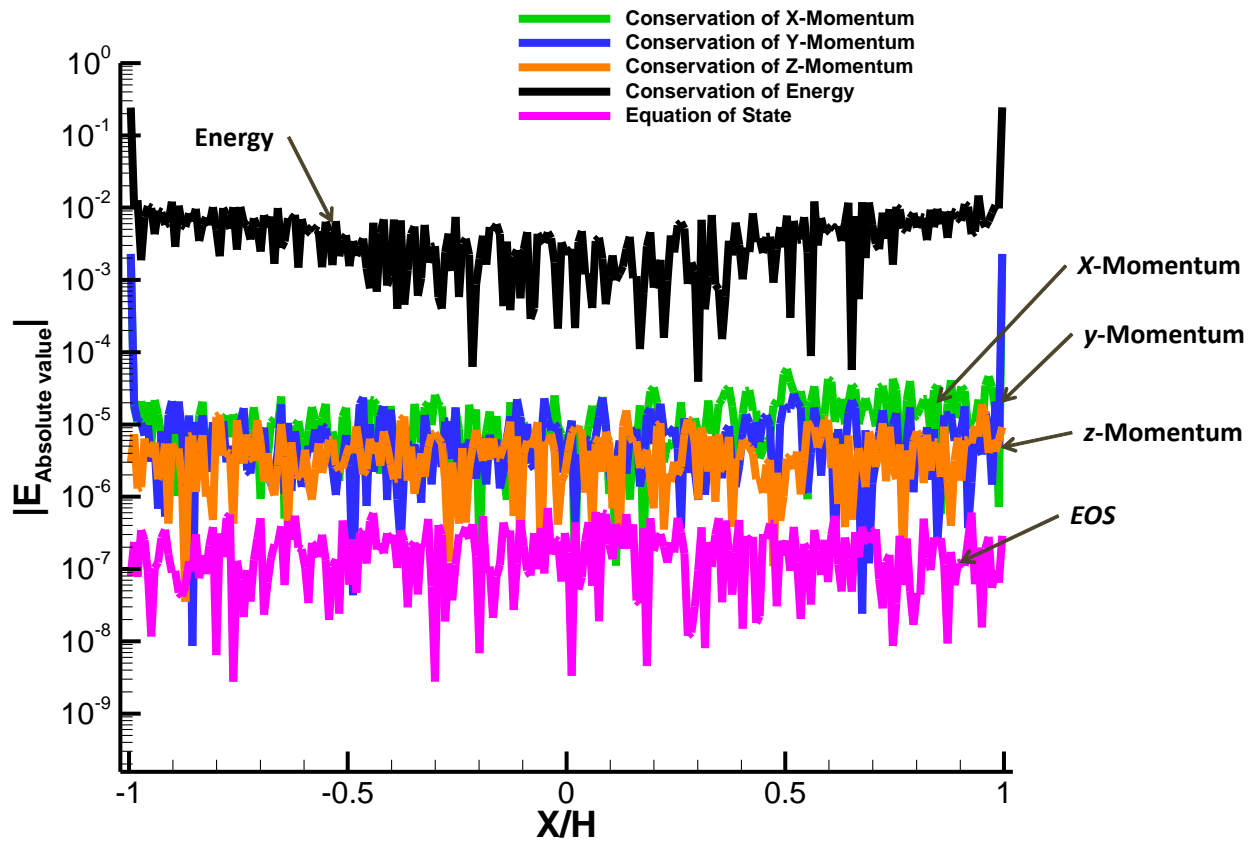
Fig. 5. Absolute (top) and normalized (bottom) errors of all conservation equations and equation of state in the compressible Couette flow problem.
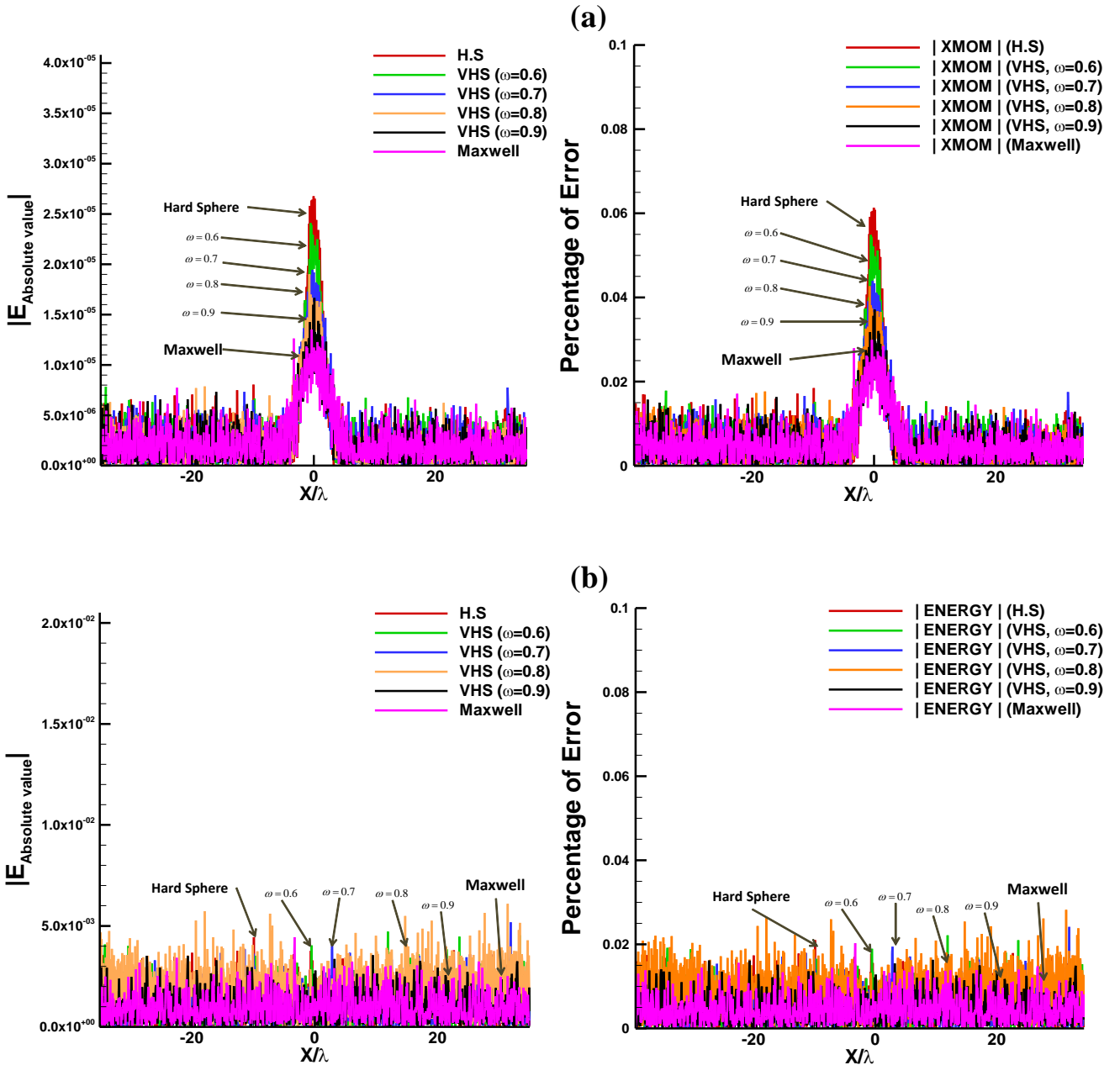
Fig. 6. The effect of different values of viscosity index on the error of conservation laws in the shock structure problem; **(a)** *x*-momentum equation, **(b)** energy equation. The vertical axis shows the order of magnitude of absolute errors (left) and normalized errors (right) based on the two norm L_2.
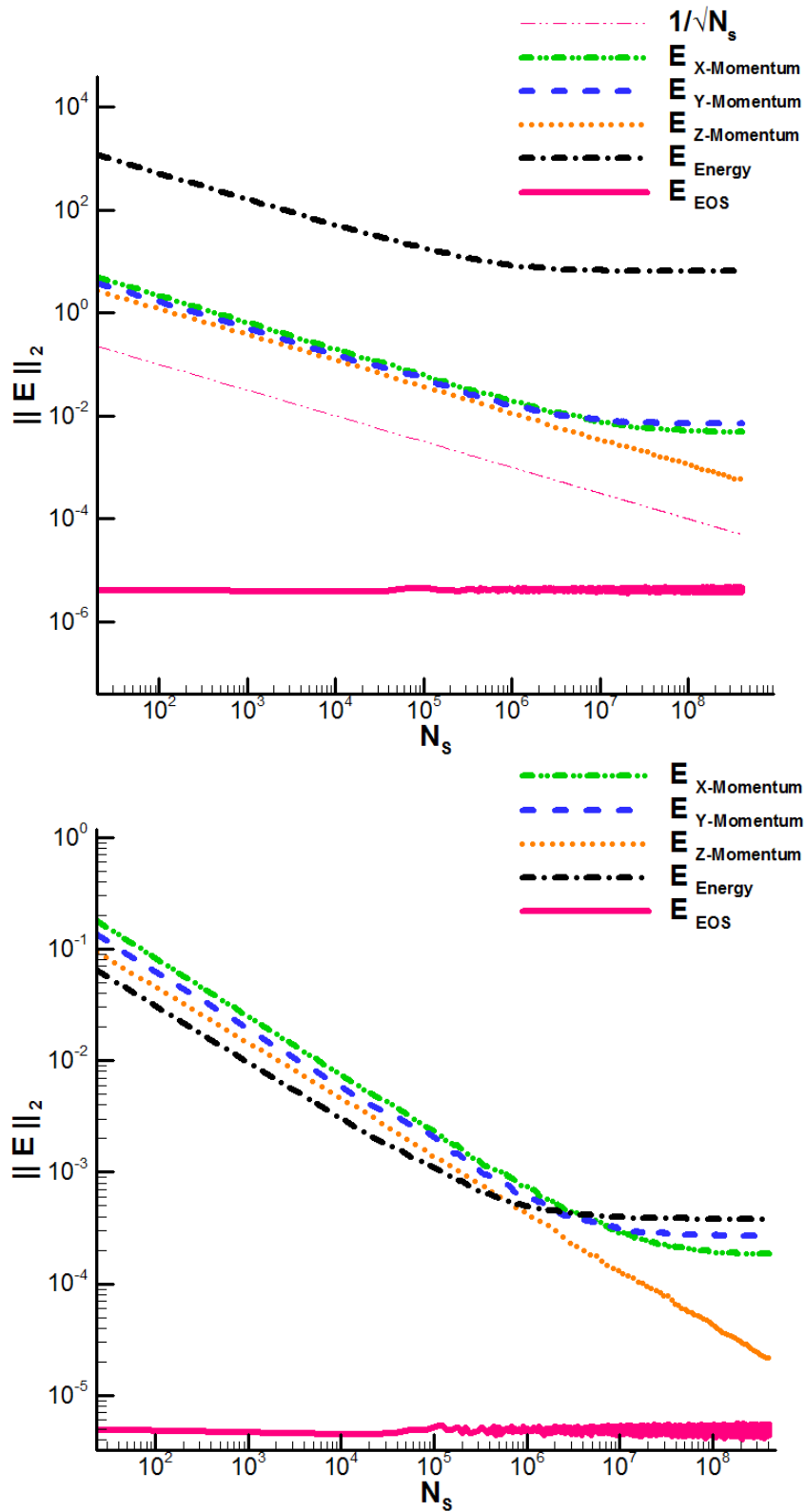
Fig. 7. The convergence history of DSMC simulation in the compressible Couette flow problem with regard to the number of sample steps. The vertical axis shows the order of magnitude of absolute errors (top) and normalized error (bottom) based on the two norm L_2.
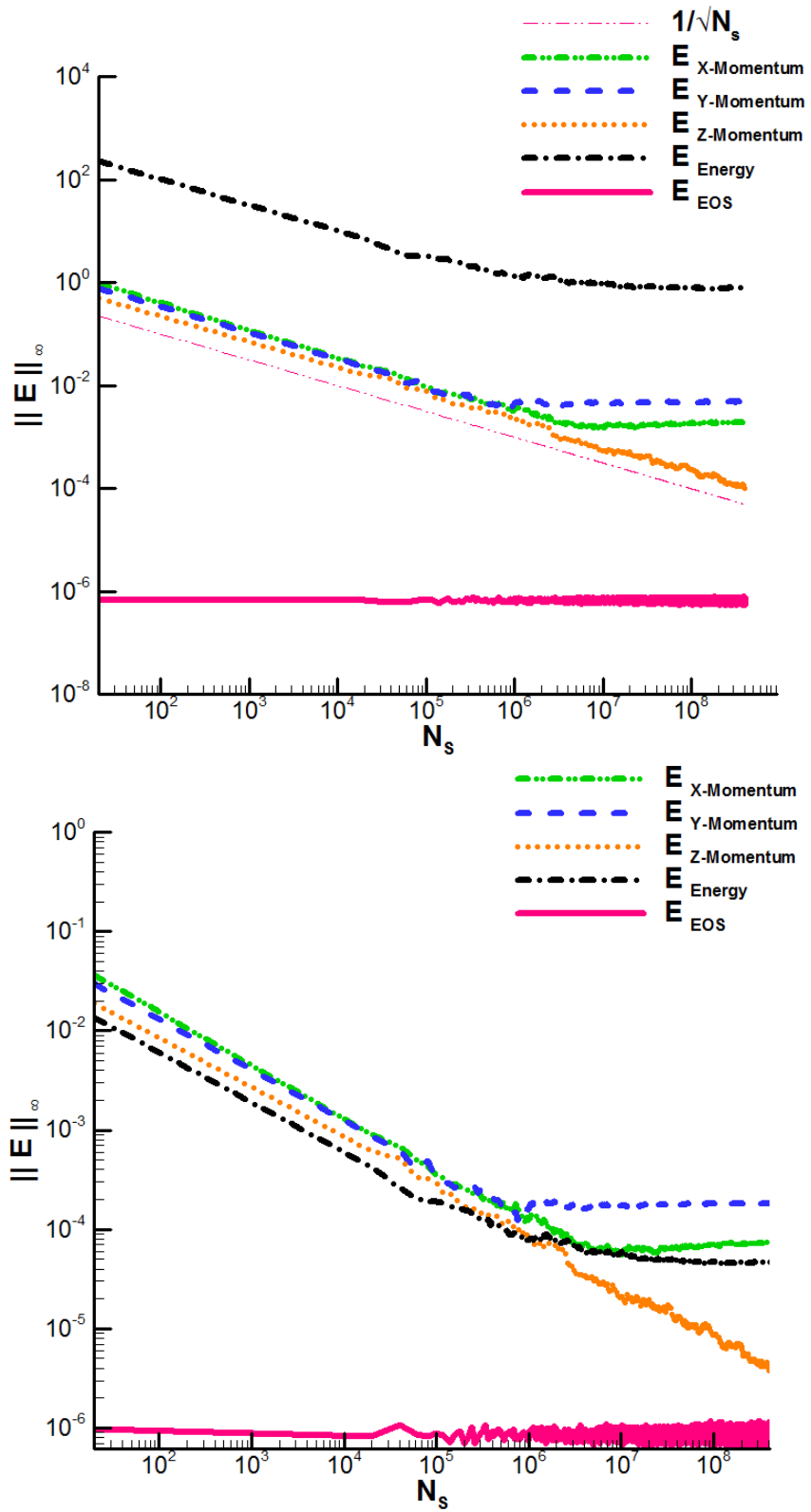
Fig. 8. The convergence history of DSMC simulation in the compressible Couette flow problem with regard to the number of sample steps. The vertical axis shows the order of magnitude of absolute errors (top) and normalized error (bottom) based on the infinity norm L_∞.
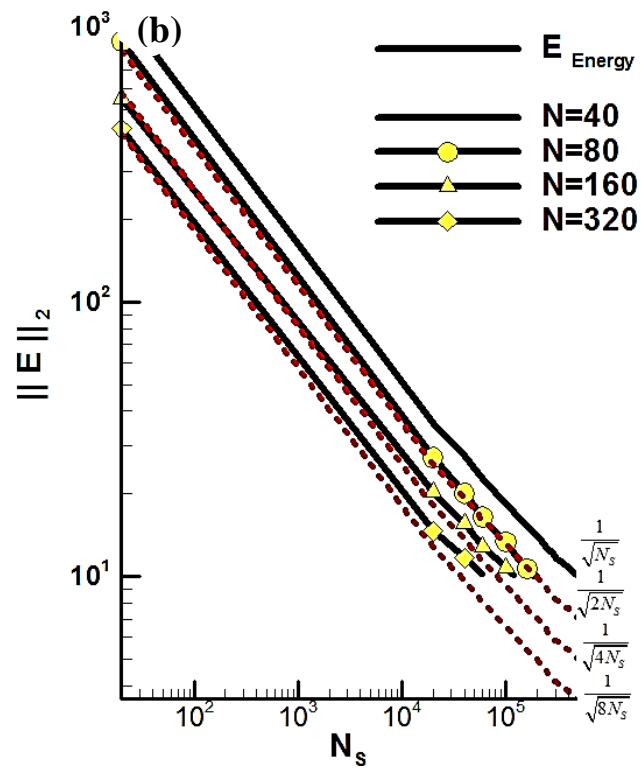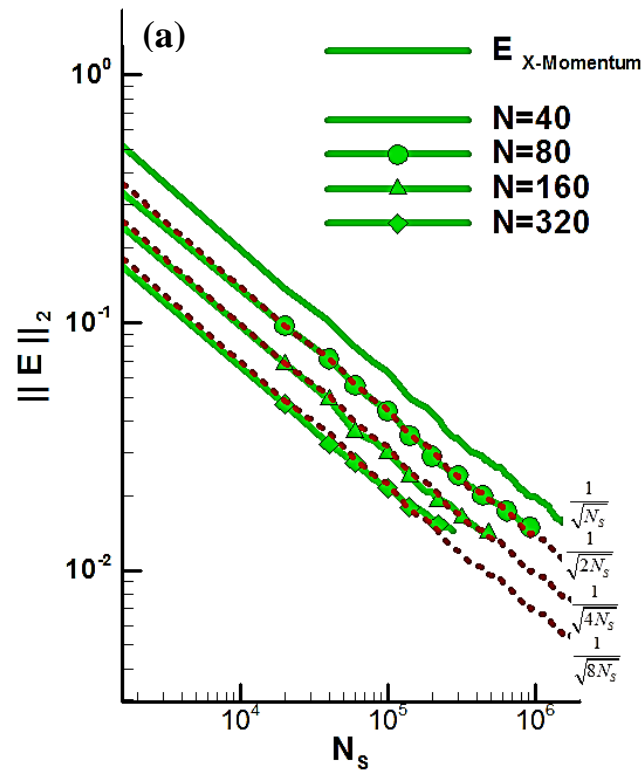
Fig. 9. The effect of number of particles on statistical behavior of convergence history in the compressible Couette flow problem; **(a)** *x*-momentum and **(b)** energy conservation equations.
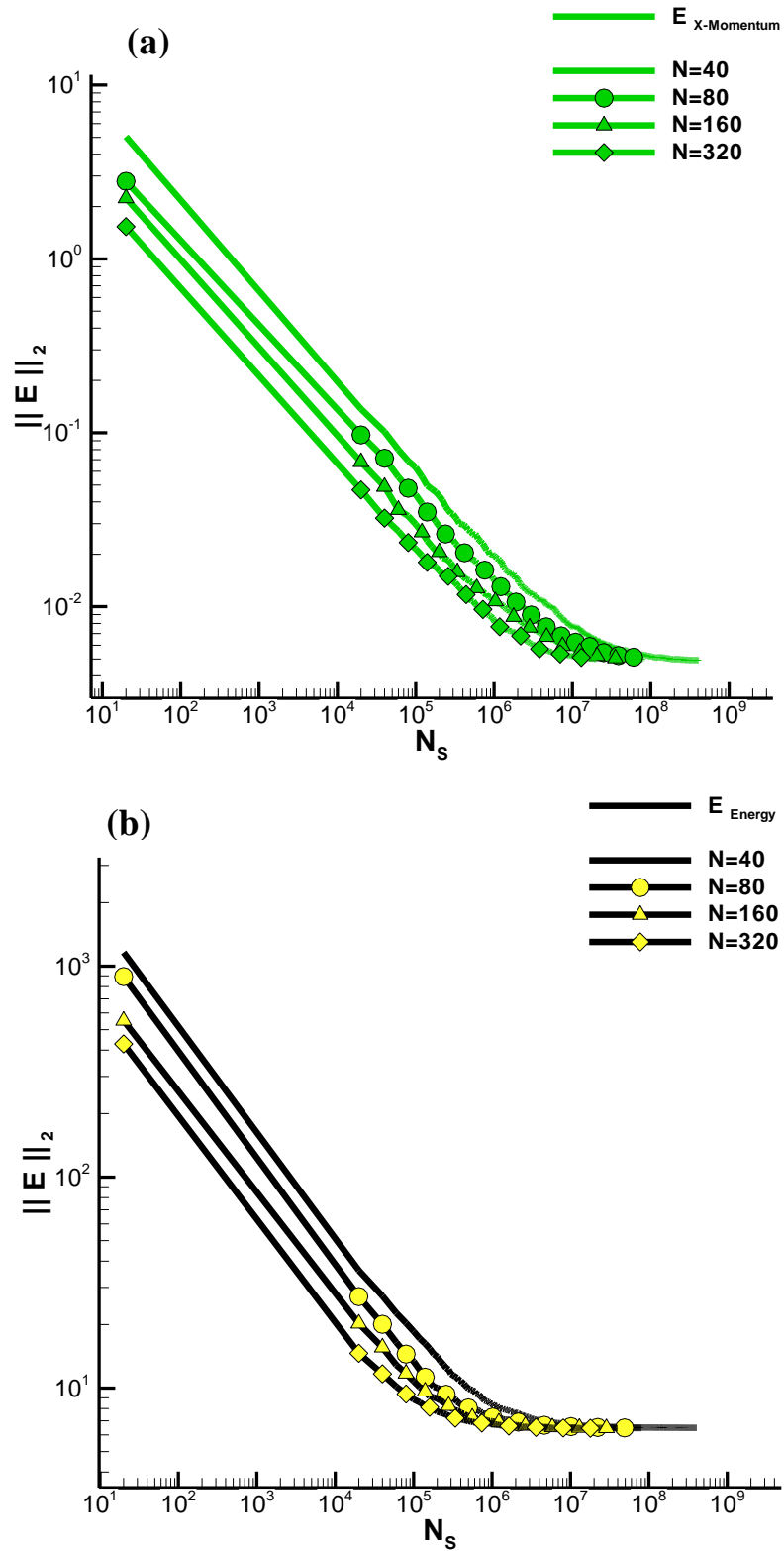
Fig. 10. The effect of number of particles on statistical behavior of convergence history in the compressible Couette flow problem, in particular, including the final stage behavior; **(a)** *x*-momentum and **(b)** energy conservation equations.
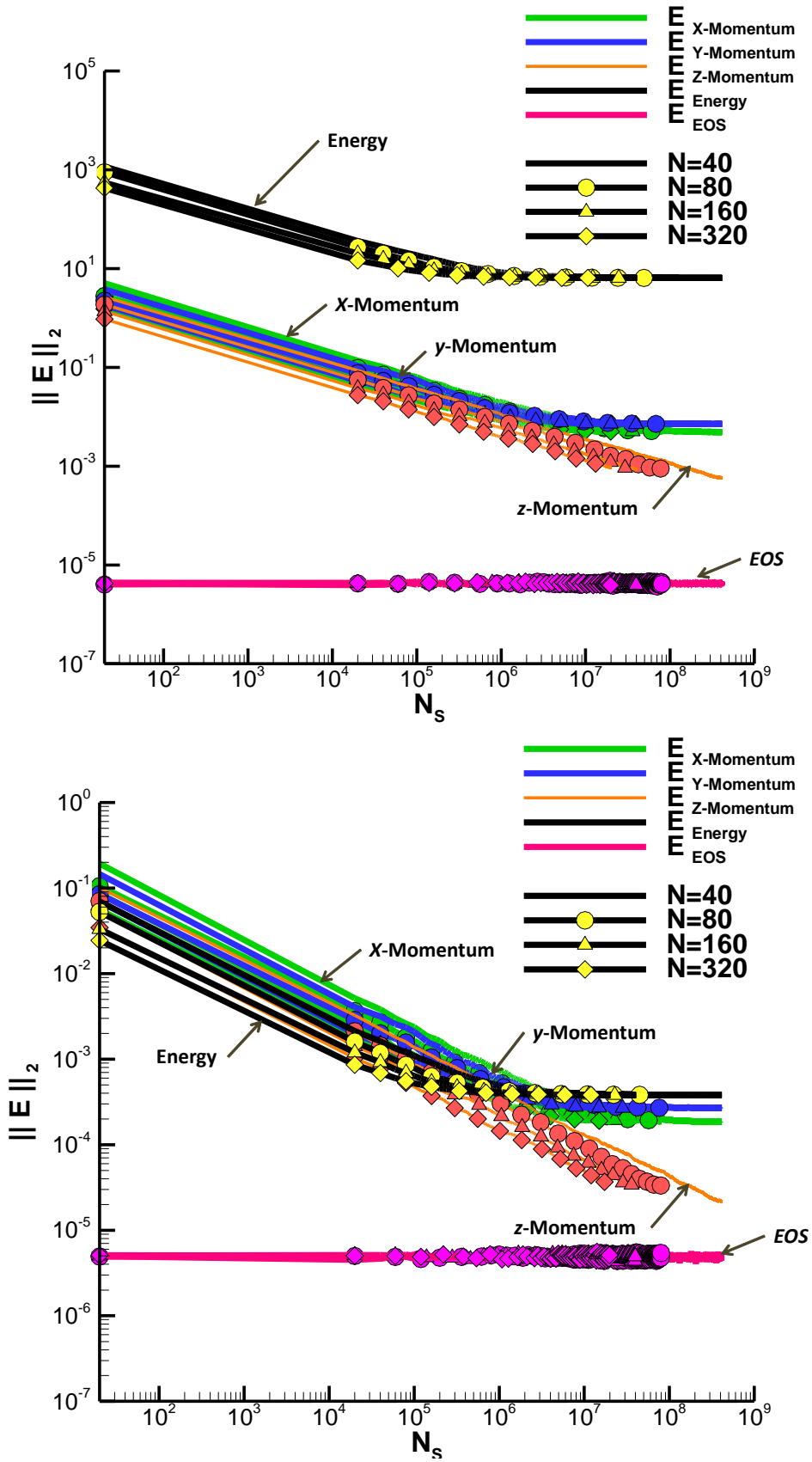
Fig. 11. The convergence history for all conservation equations and equation of state for different number of particles in the compressible Couette flow problem. The vertical axis shows the order of magnitude of absolute errors (top) and normalized error (bottom) based on the two norm L_2.

40
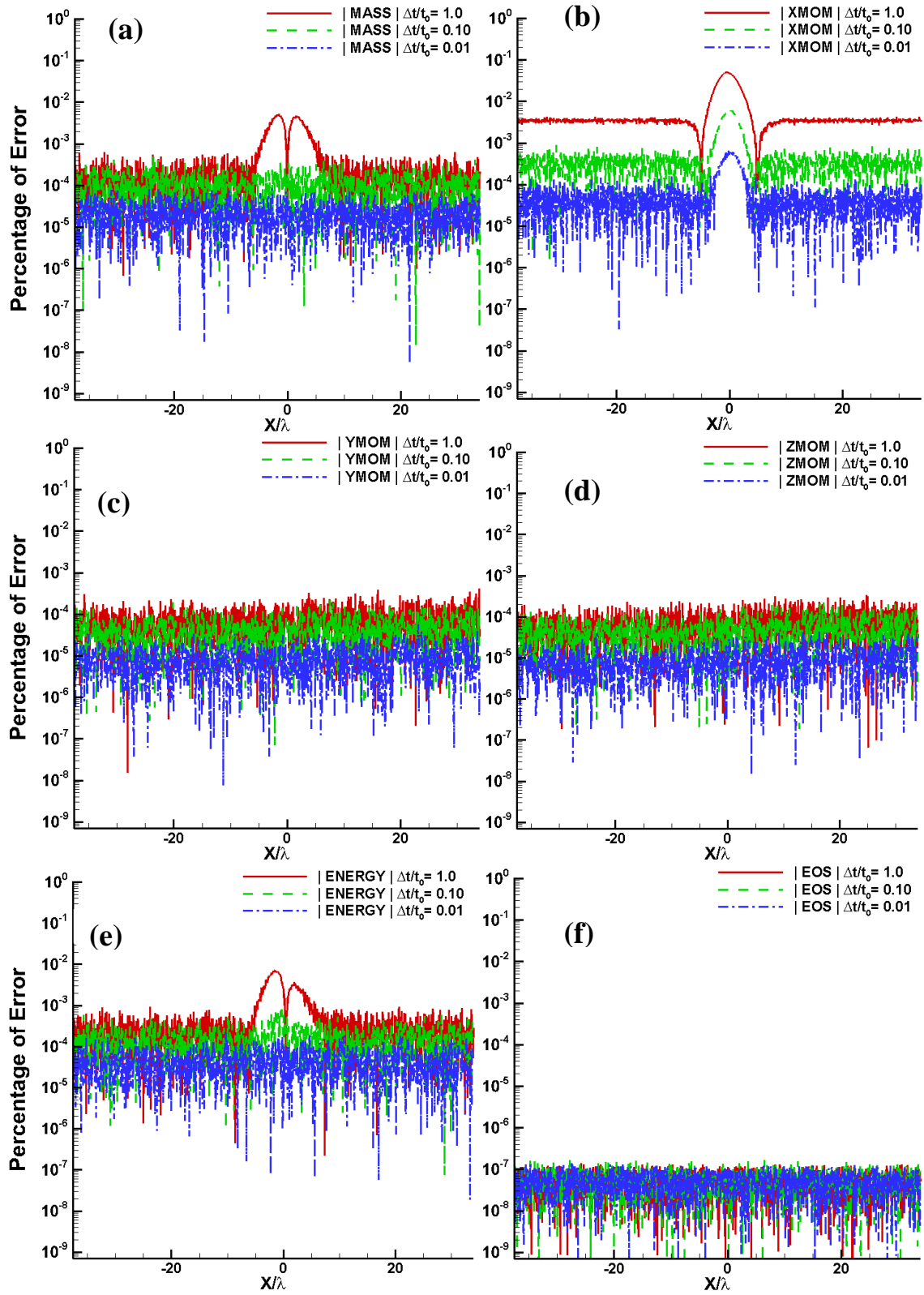
Fig. 12. The effect of time-step size on normalized errors percentages in the shock structure problem; **(a)** mass, **(b)** *x*-momentum, **(c)** *y*-momentum, **(d)** *z*-momentum, **(e)** energy conservation equations and **(f)** equation of state.
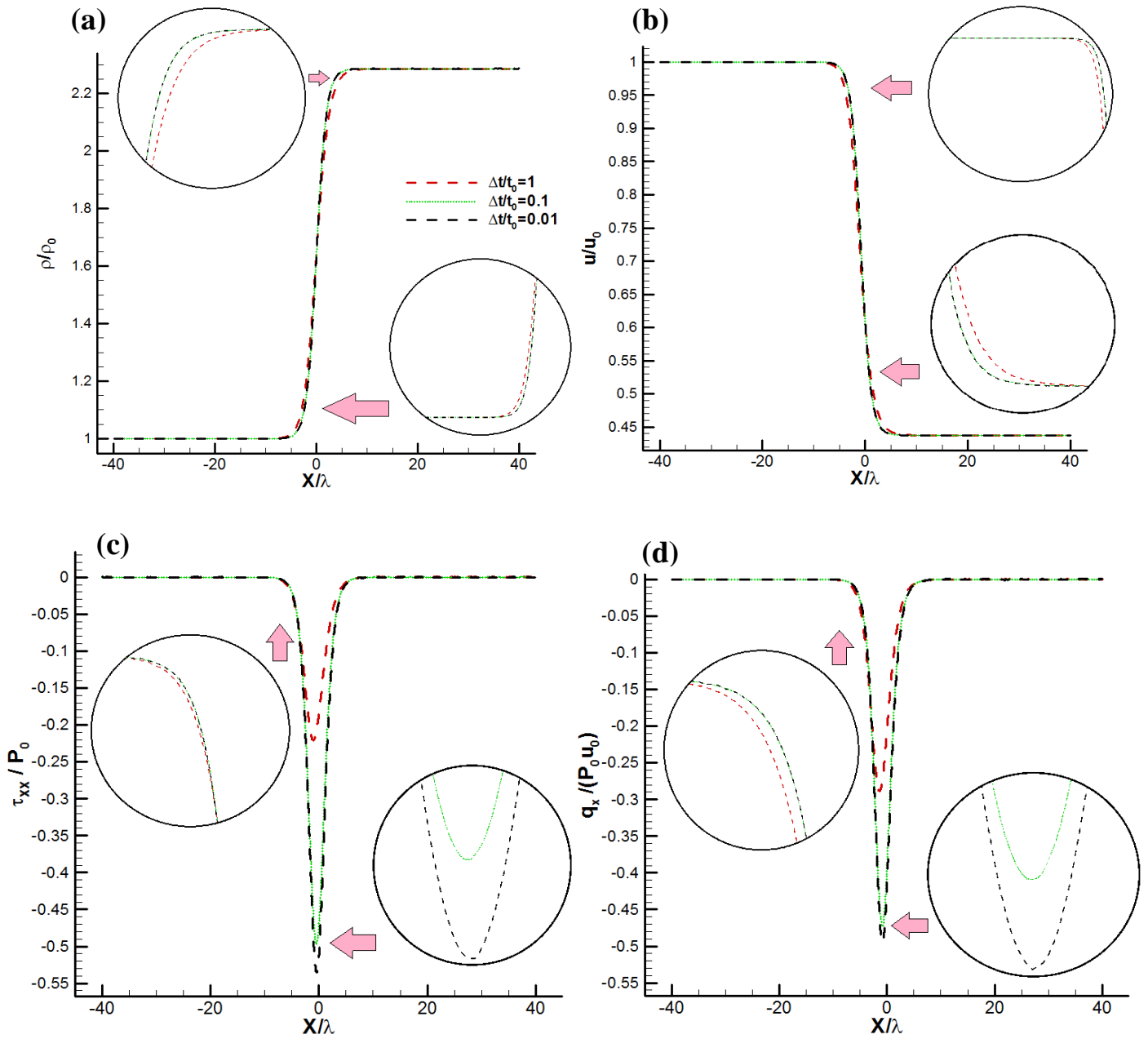
Fig. 13. The shock structure profiles in case with different values of Δt ; **(a)** density, **(b)** velocity, **(c)** normal stress, and **(d)** heat flux.
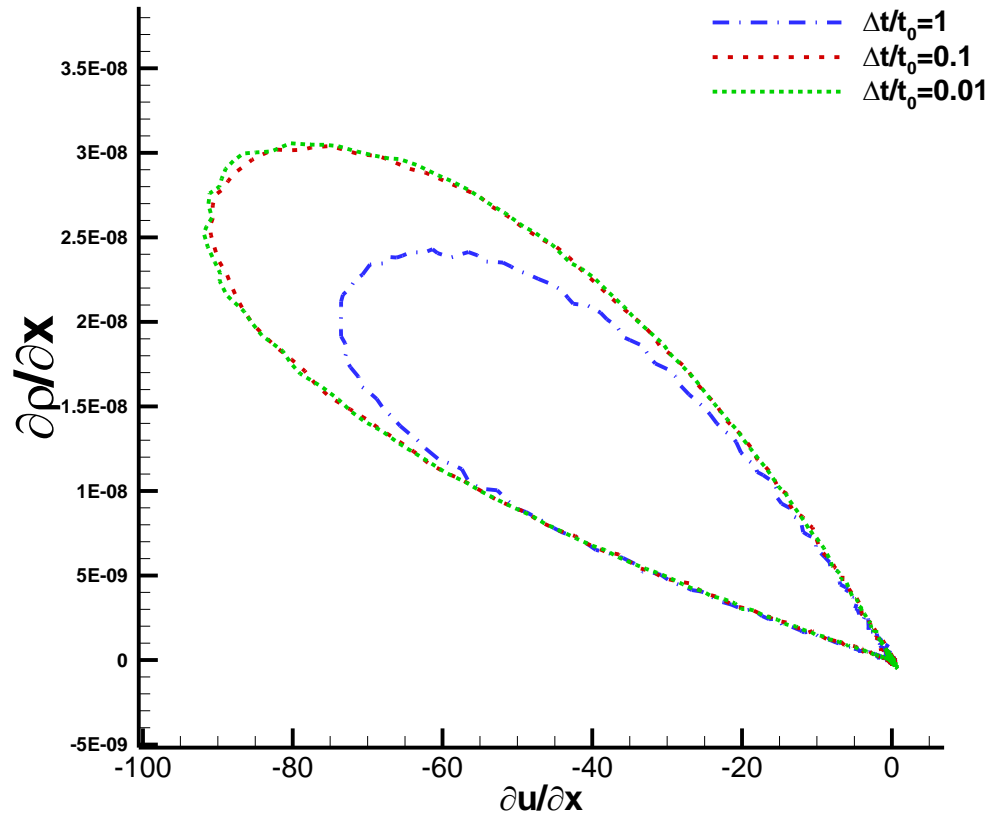
Fig. 14. The effect of time-step size on the gradient of the hydrodynamic variables in the shock structure problem (the velocity gradient versus the density gradient).
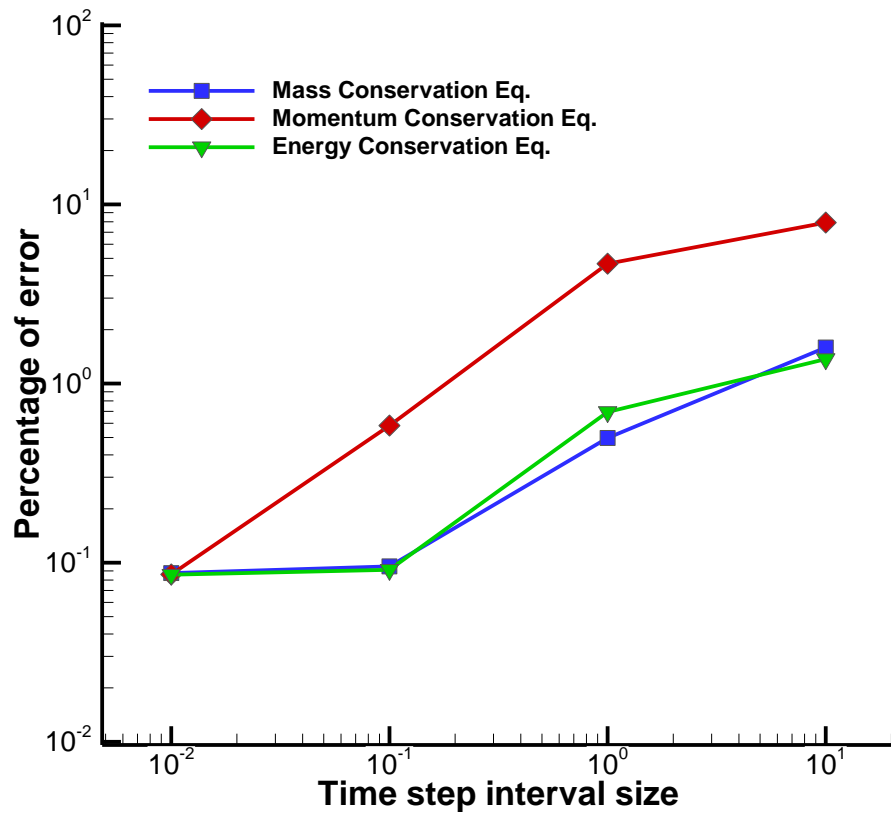
Fig. 15. The percentage of relative errors for four different time steps.
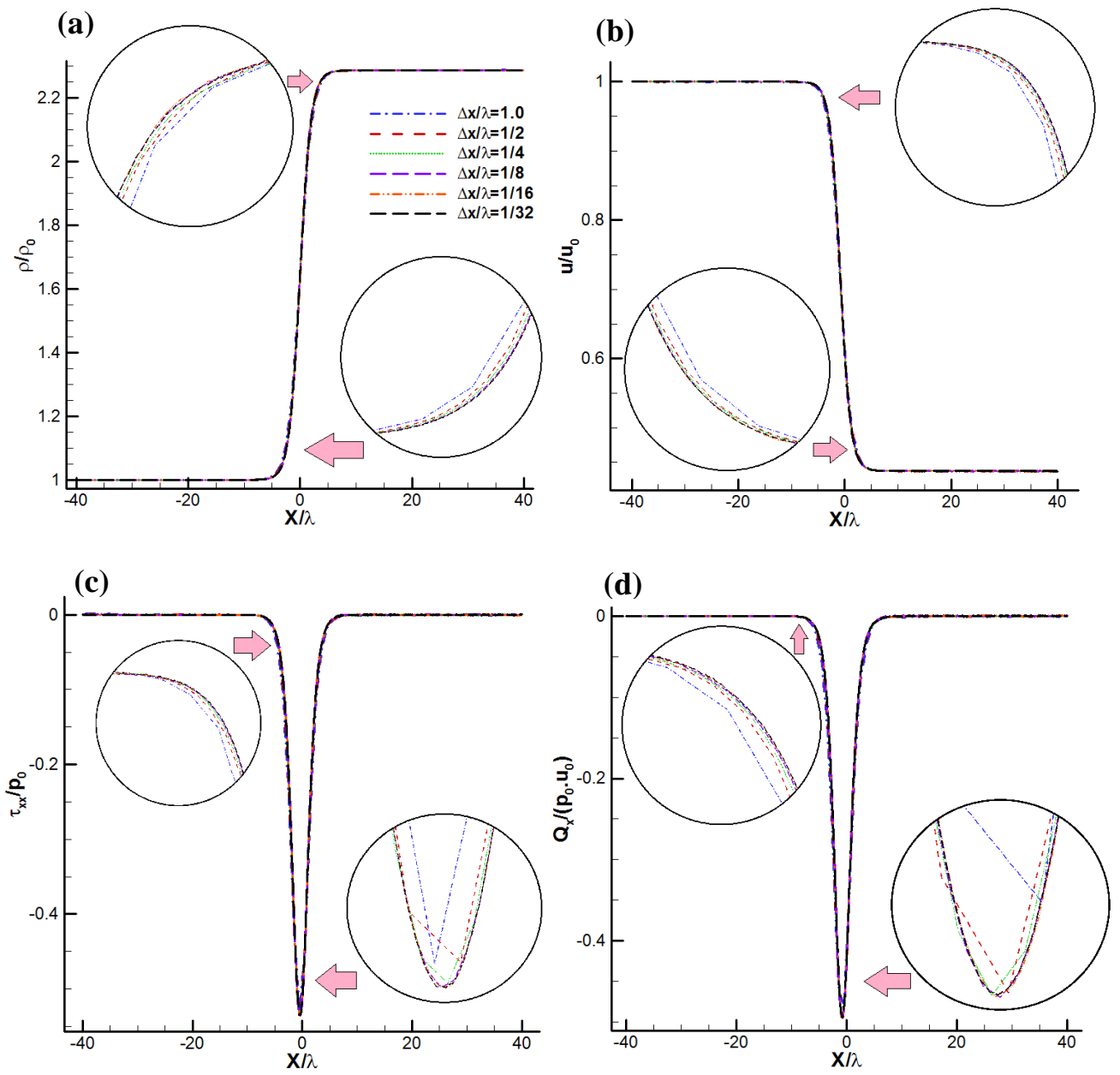
Fig. 16. The shock structure profiles in case with different values of cell length size; **(a)** density, **(b)** velocity, **(c)** normal stress, and **(d)** heat flux.
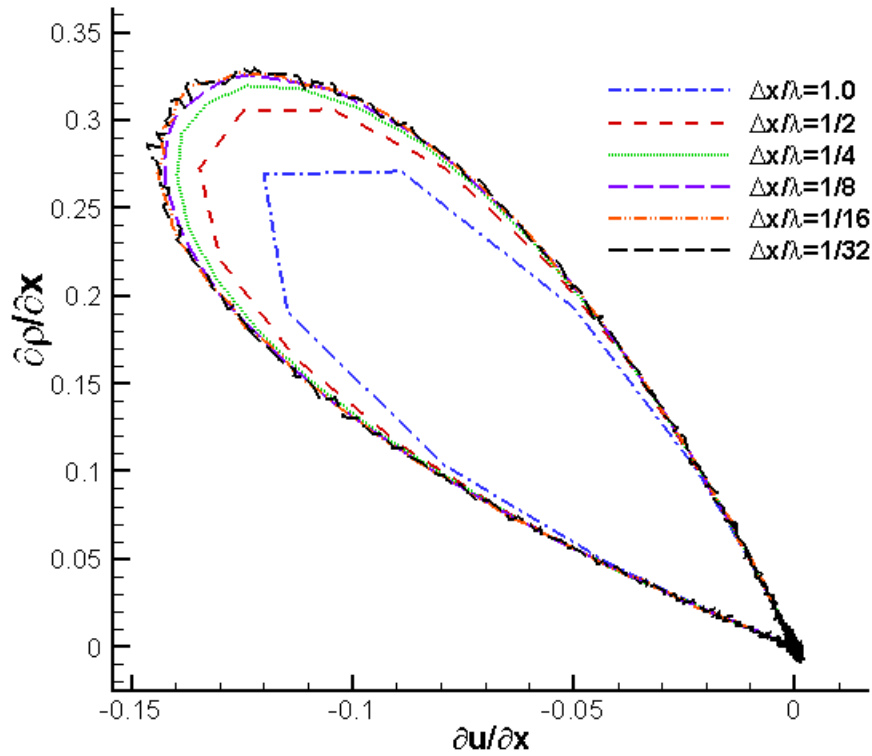
Fig. 17. The effect of cell size on the gradient of the hydrodynamic variables in the shock structure problem (the velocity gradient versus the density gradient).
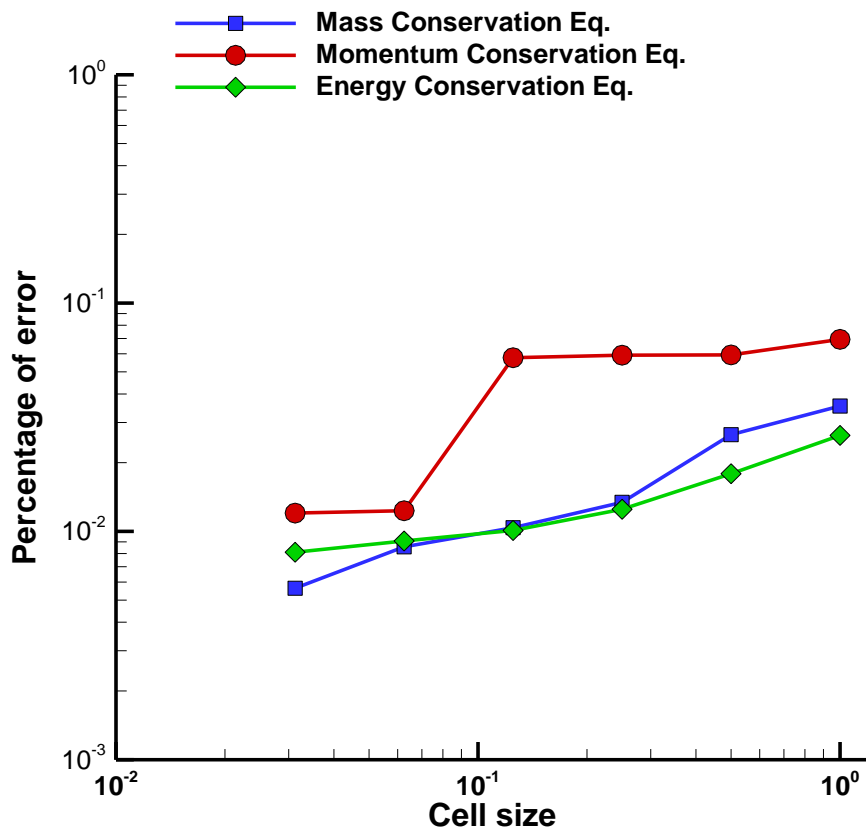
Fig. 18. The percentage of relative errors for different cell length sizes.
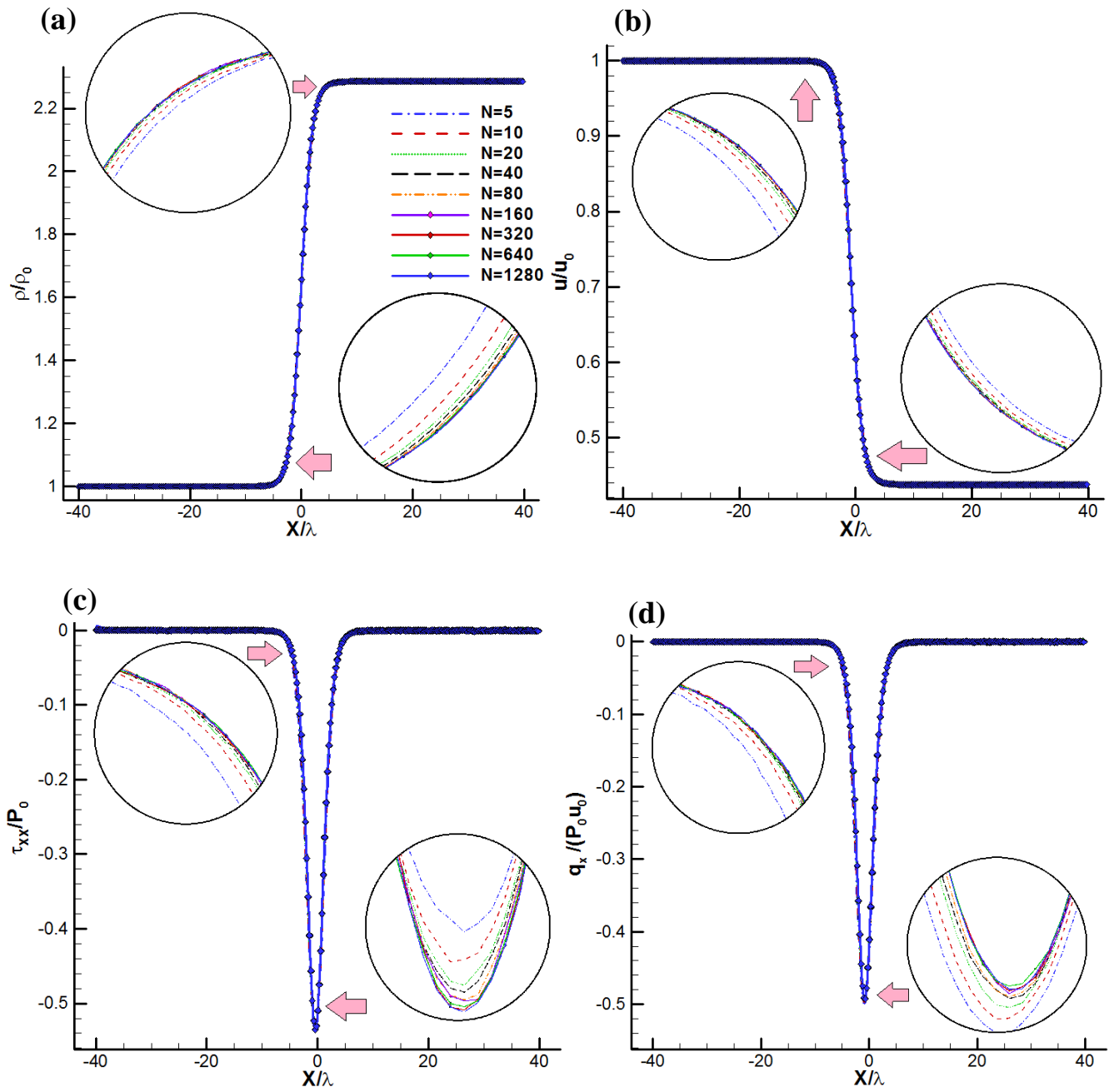
Fig. 19. The shock structure profiles in case with different number of particles; **(a)** density, **(b)** velocity, **(c)** normal stress, and **(d)** heat flux.
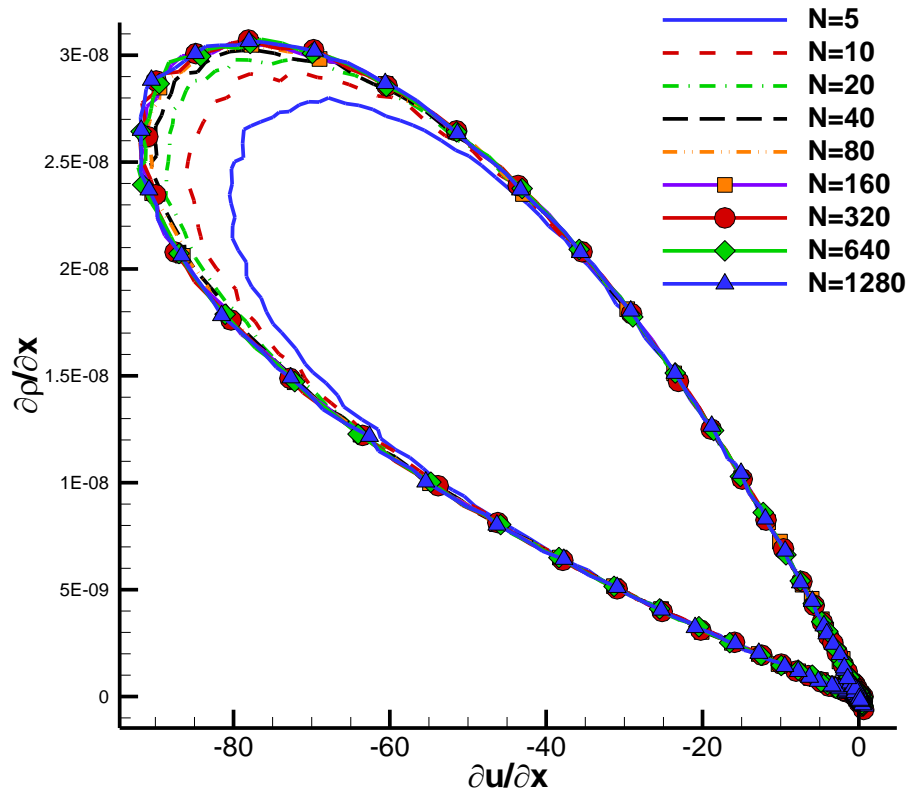
Fig. 20. The effect of number of particles on the gradient of the hydrodynamic variables in the shock structure problem (the velocity gradient versus the density gradient).
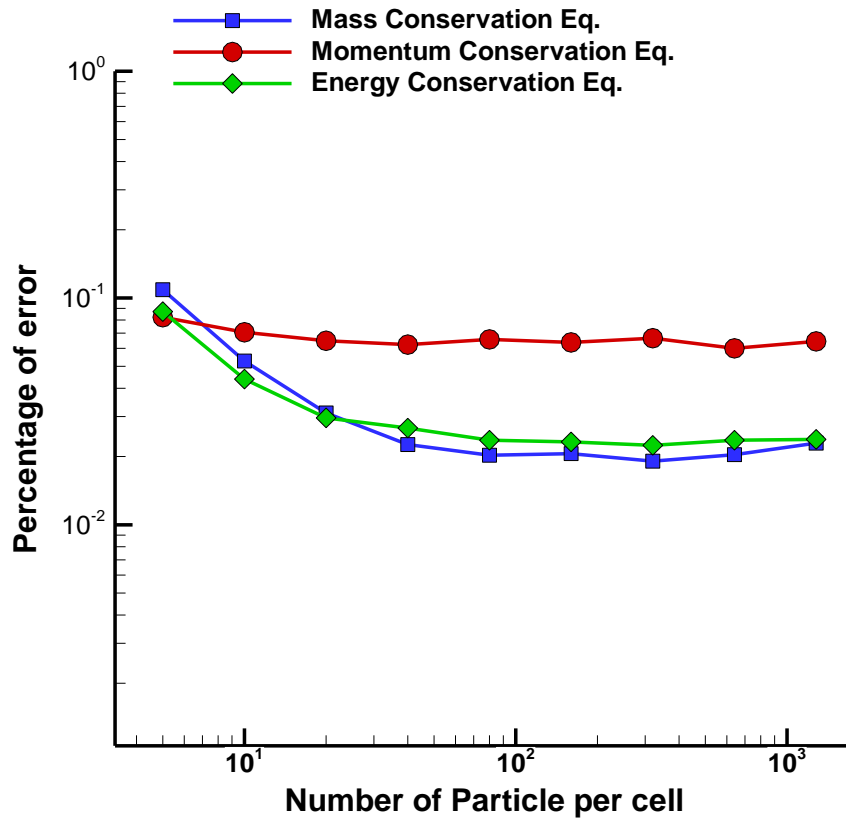
Fig. 21. The percentage of error for different number of particles per cell.